3. **Andreakos E,** Foxwell B, Feldmann M. Is targeting Toll-like receptors and their signaling pathway a useful therapeutic approach to modulating cytokine-driven inflammation? *Immunol Rev* 2004;**202**:250–65.
4. **Kang SSW,** Kauls LS, Gaspari AA. Toll-like receptors: applications to dermatologic disease. *J Am Acad Dermatol* 2006;**54**:951–83.
5. **Lehner T,** Lavery E, Smith R, van der Zee R, Mizushima Y, Shinnick T. Association between the 65-kilodalton heat shock protein, Streptococcus sanguis, and the corresponding antibodies in Behçet's syndrome. *Infect Immun* 1991;**59**:1434–41.
6. **Pervin K,** Childerstone A, Shinnick T, Mizushima Y, van der Zee R, Hasan A, *et al*. T cell epitope expression of mycobacterial and homologous human 65-kilodalton heat shock protein peptides in short term cell lines from patients with Behçet's disease. *J Immunol* 1993;**151**:2273–82.
7. **Direskeneli H,** Hasan A, Shinnick T, Mizushima R, van der Zee R, Fortune F, *et al*. Recognition of B-cell epitopes of the 65 kDa HSP in Behçet's disease. *Scand J Immunol* 1996;**43**:464–71.
8. **Kaneko S,** Suzuki N, Yamashita N, Nagafuchi H, Nakajima T, Wakisaka S, *et al*. Characterization of T cells specific for an epitope of human 60-kD heat shock protein (hsp) in patients with Behçet's disease (BD) in Japan. *Clin Exp Immunol* 1997;**108**:204–12.
9. **Mege JL,** Dilsen N, Sanguedolce V, Gul A, Bongrand P, Roux H, *et al*. Overproduction of monocyte derived tumor necrosis factor α, interleukin (IL) 6, IL-8 and increased neutrophil superoxide generation in Behçet's disease. A comparative study with familial Mediterranean fever and healthy subjects. *J Rheum* 1993;**20**: 1544–9.

Expression of high mobility group protein 1 in the sera of patients and mice with systemic lupus erythematosus

High mobility group protein 1 (HMGB1) is a non-histone nuclear protein with a dual function. Inside the cell, HMGB1 binds to DNA and modulates a variety of processes, including transcription. Outside the cell, HMGB1 can serve as an alarmin to mediate disease manifestations in animal models of sepsis and arthritis; in these models, blocking HMGB1 can attenuate disease.[1–3]

In *in vitro* experiments, HMGB1 translocation and cellular release can occur during activation as well as cell death and is present in tissue in conditions, such as rheumatoid arthritis and cutaneous lupus.[4 5] While original studies suggested that release occurs only with necrosis,[6] more recent studies have shown that HMGB1 release also occurs in late apoptosis.[7 8] As increased apoptosis and decreased clearance of apoptotic material may underlie the pathogenesis of systemic lupus erythematosus (SLE), these findings suggest that extracellular HMGB1 levels rise in this disease and promote systemic and local inflammation.

To elucidate the expression of HMGB1 in SLE, we have investigated blood levels of HMGB1, using Western blotting to analyse serum samples from a murine lupus model and patients with SLE. We obtained serum samples from MRL/MpJ-*lpr/lpr* and BALB/c mice purchased from the Jackson Laboratory (Bar Harbor, MA, USA). Human SLE serum samples were purchased from Immunovision (Springdale, AR, USA). For Western blotting, electrophoresis was performed using a 4–12% Bis-Tris sodium dodecyl sulphate–polyacrylamide gel electrophoresis (Invitrogen, San Diego, CA, USA). Protein was transferred on to PDVF membrane and blotted with a rabbit anti-HMGB1 polyclonal antiserum (gift of Dr Kevin Tracey, North-Shore Jewish Hospital, Long Island, NY, USA) followed by HRP-conjugated anti-rabbit IgG and Super Signal West Femto substrate (Pierce, Rockford, IL, USA). Images were captured with a CCD camera.

As data in fig 1 indicate, sera from patients with SLE as well as MRL/MpJ-*lpr/lpr* mice show increased levels of HMGB1 by Western blotting. To assess the extent of this increase, the density of the HMGB1 band was analysed by AlphaEasyFC version 3.1.2 and the value expressed as fold increase over control. In samples studied, for human sera, the amounts of HMGB1 increased 2.8–36-fold while, for the murine sera, the values increase 1–28-fold over controls. Furthermore, in MRL/MpJ-*lpr/lpr* mice, the HMGB1 levels rose with disease progression (data not shown). Together, these data indicate that HMGB1 release occurs with SLE and can produce increased levels in the sera similar to that occurs in sepsis and shock.[2 9] Further analysis will be need to determine the relationship to disease activity and treatment.

In the context of SLE, increased levels of other nuclear constituents in the blood (eg, DNA) have been attributed to cell death, with impaired clearance mechanisms (eg, complement deficiency) preventing normal disposal. Extracellular HMGB1 in

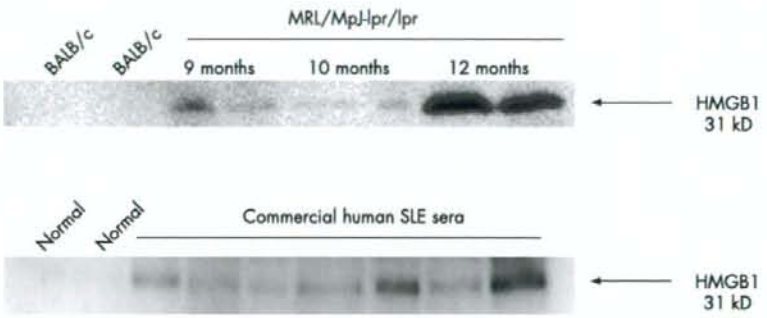

Figure 1 Detection of high mobility group protein 1 (HMGB1) in mouse and human sera. Sera from either mice (A) or human (B) were resolved on sodium dodecyl sulphate–polyacrylamide gel electrophoresis and analysed by Western blotting with an anti-HMGB1 antibody. SLE, systemic lupus erythematosus.

nature genetics

Susceptibility loci for intracranial aneurysm in European and Japanese populations

Kaya Bilguvar[1,2], Katsuhito Yasuno[3], Mika Niemelä[4], Ynte M Ruigrok[5], Mikael von und zu Fraunberg[6], Cornelia M van Duijn[7], Leonard H van den Berg[5], Shrikant Mane[8], Christopher E Mason[2,9], Murim Choi[2], Emília Gaál[1,2,4], Yasar Bayri[1,2], Luis Kolb[1,2], Zulfikar Arlier[1,2], Sudhakar Ravuri[8], Antti Ronkainen[6], Atsushi Tajima[3], Aki Laakso[4], Akira Hata[10], Hidetoshi Kasuya[11], Timo Koivisto[6], Jaakko Rinne[6], Juha Öhman[12], Monique M B Breteler[7], Cisca Wijmenga[13,14], Matthew W State[2,9], Gabriel J E Rinkel[5], Juha Hernesniemi[4], Juha E Jääskeläinen[6], Aarno Palotie[15,16], Ituro Inoue[3], Richard P Lifton[2,17] & Murat Günel[1,2]

Stroke is the world's third leading cause of death. One cause of stroke, intracranial aneurysm, affects ~2% of the population and accounts for 500,000 hemorrhagic strokes annually in mid-life (median age 50), most often resulting in death or severe neurological impairment[1]. The pathogenesis of intracranial aneurysm is unknown, and because catastrophic hemorrhage is commonly the first sign of disease, early identification is essential. We carried out a multistage genome-wide association study (GWAS) of Finnish, Dutch and Japanese cohorts including over 2,100 intracranial aneurysm cases and 8,000 controls. Genome-wide genotyping of the European cohorts and replication studies in the Japanese cohort identified common SNPs on chromosomes 2q, 8q and 9p that show significant association with intracranial aneurysm with odds ratios 1.24–1.36. The loci on 2q and 8q are new, whereas the 9p locus was previously found to be associated with arterial diseases, including intracranial aneurysm[2–5]. Associated SNPs on 8q likely act via *SOX17*, which is required for formation and maintenance of endothelial cells[6–8], suggesting a role in development and repair of the vasculature; *CDKN2A* at 9p may have a similar role[9]. These findings have implications for the pathophysiology, diagnosis and therapy of intracranial aneurysm.

Siblings of intracranial aneurysm probands are at ~fourfold increased risk of hemorrhage from intracranial aneurysm, suggesting a genetic component to risk[10]. Genome-wide linkage studies of familial cases[11] and rare apparently mendelian kindreds have not thus far identified robustly replicable loci, and no underlying mutations have been identified[12–14]. Similarly, examination of candidate genes in small case-control studies has failed to produce replicable results[12].

These considerations motivate the use of GWAS to identify common variants that contribute to intracranial aneurysm. We carried out a multistage intracranial aneurysm GWAS in three cohorts: a Finnish cohort of 920 cases and 985 controls, a Dutch cohort of 781 cases and 6,424 controls and a Japanese cohort of 495 cases and 676 controls (see **Supplementary Methods** online).

The study design consisted of a first stage of genome-wide genotyping of the European cohorts on the Illumina platform, careful matching of cases and controls, and identification of intervals harboring SNPs that surpassed a significance threshold of 5×10^{-7} for association with intracranial aneurysm[2]. This discovery phase had 80% power to detect common alleles that confer a genotype relative risk (GRR) of 1.31 and 50% power to detect a GRR of 1.25 (assuming an additive model in log-odds scale). Replication of association of SNPs in these intervals was tested in the Japanese cohort, setting $P < 0.05$ for significant replication. The replication study had

[1]Departments of Neurosurgery, Neurobiology and [2]Genetics, Yale Program on Neurogenetics, Yale Center for Human Genetics and Genomics, Yale University School of Medicine, New Haven, Connecticut 06510, USA. [3]Division of Molecular Life Science, School of Medicine, Tokai University, Shimokasuya 143, Isehara, Kanagawa 259-1193, Japan. [4]Department of Neurosurgery, Helsinki University Central Hospital, Helsinki, P.O. Box 266, FI-00029 HUS, Finland. [5]Department of Neurology, Rudolf Magnus Institute of Neuroscience, University Medical Center Utrecht, 3584 CX Utrecht, The Netherlands. [6]Department of Neurosurgery, Kuopio University Hospital, Kuopio FI-70211, Finland. [7]Genetic Epidemiology Unit, Department of Epidemiology and Biostatistics and Department of Clinical Genetics, Erasmus Medical Center, 2040, 3000 CA Rotterdam, The Netherlands. [8]Keck Foundation Biotechnology Resource Laboratory, Yale University, 300 George Street, New Haven, Connecticut 06510, USA. [9]Child Study Center, Yale University School of Medicine, New Haven, Connecticut 06510, USA. [10]Department of Public Health, School of Medicine, Chiba University, Chiba 260-8670, Japan. [11]Department of Neurosurgery, Medical Center East, Tokyo Women's University, Tokyo 116-8567, Japan. [12]Department of Neurosurgery, Tampere University Hospital, 33521 Tampere, Finland. [13]Complex Genetics Section, Department of Biomedical Genetics, University Medical Center Utrecht, 3508 AB Utrecht, The Netherlands. [14]Department of Genetics, University Medical Center Groningen and University of Groningen, 9700 RR Groningen, The Netherlands. [15]Biomedicum Helsinki, Research Program in Molecular Medicine, University of Helsinki, 00290 Helsinki, Finland. [16]Wellcome Trust Sanger Institute, Wellcome Trust Genome Campus, Hinxton, Cambridge CB10 1HH, UK. [17]Howard Hughes Medical Institute and Department of Internal Medicine, Yale University School of Medicine, New Haven, Connecticut 06510, USA. Correspondence should be addressed to R.P.L. (richard.lifton@yale.edu) or M.G. (murat.gunel@yale.edu).

Received 7 July; accepted 18 August; published online 9 November 2008; doi:10.1038/ng.240

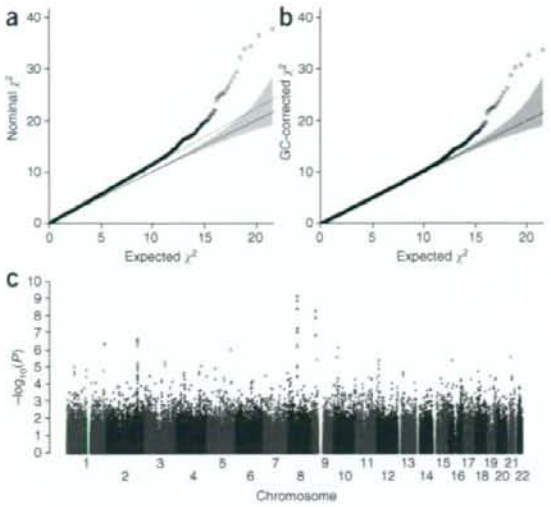

Figure 1 Genome-wide association of SNPs with intracranial aneurysm in the combined European cohort. (**a**) Quantile-quantile plot of the observed χ^2 values derived from the Mantel-extension test statistics versus the expected χ^2 distribution. The solid line represents concordance of observed and expected values. The slope of the dashed line represents the genomic inflation factor ($\lambda = 1.11$). (**b**) The plot of expected and observed χ^2 values for association of SNPs with intracranial aneurysm after correction for the genomic inflation factor ($\lambda = 1.0$). Significant deviation from the expected values suggests association of these SNPs with intracranial aneurysm phenotype. (**c**) The $-\log_{10}$ of uncorrected P values for association of each SNP and intracranial aneurysm is plotted according to its physical position on successive chromosomes. Green dots indicate SNPs yielding P values $<1 \times 10^{-5}$, and red dots denote SNPs that surpass a significance level of 5×10^{-7}.

80% and 66% power to replicate SNPs with GRRs of 1.31 and 1.25, respectively. The utility of using a genetically diverse population for replication has been demonstrated by recent studies[15], thereby extending association results to a broad segment of the world's population.

Discovery phase genotypes were processed using rigorous quality controls; because Dutch controls and some Finnish controls were genotyped separately on Illumina chips of varying SNP density, particular attention was paid to ensuring consistent genotyping performance and excluding nonrandom genotyping error within and across cohorts (**Supplementary Methods** and **Supplementary Tables 1** and **2** online). To control for population stratification, we genetically matched cases and controls from each cohort[16], resulting in a dataset in which cases and controls are similarly distributed along axes of significant principal components (**Supplementary Table 1**).

We tested for association between each SNP and intracranial aneurysm by using the Cochran-Armitage trend test in each cohort and combined the results using the Mantel extension test. The distribution of test statistics for association of SNPs with intracranial aneurysm in the combined cohort is shown in **Figure 1a**. The genomic inflation factor (λ) was 1.043 and 1.136 for the Finnish and Dutch, respectively, and 1.114 combined, indicating well-matched populations[17] (**Fig. 1a**); further logistic regression including principal components as covariates[2] did not significantly change λ (**Supplementary Fig. 1** online), nor did exclusion of SNPs with call rates <99% in any case or control cohort (**Supplementary Methods**); in contrast, because genomic inflation factor increases with sample size[18], the large Dutch control sample was a major contributor to λ (**Supplementary Methods**). The association results reveal a number of SNPs whose P values exceed those expected under the null hypothesis; these persist after correction for λ (**Fig. 1b**). The P values across each chromosome are shown in **Figure 1c**. Four intervals (on 1q, 2q, 8q and 9p) harbored SNPs that surpassed the threshold for genome-wide significance; these include multiple SNPs with correlated P values and comprise 15 of the 16 SNPs with $P < 10^{-6}$ (**Fig. 1c**). Associated SNPs in each interval have very high call rates in every cohort and none violate HWE in any cohort (**Supplementary Table 2**). The first three loci have not previously shown association with intracranial aneurysm or other diseases, whereas SNPs on 9p are in the block of linkage disequilibrium (LD) that has previously been shown to be associated with myocardial infarction[2–4], abdominal aortic aneurysm and intracranial aneurysm[5]. Both Finnish and Dutch cohorts contributed to the significance of each locus, the risk alleles were identical and their odds ratios were not significantly different between cohorts (**Table 1**).

To attempt to replicate these four loci, we genotyped 15 SNPs from these intervals in the Japanese cohort (**Supplementary Tables 2** and **3** online). Eight of the 15 SNPs showed significant association with intracranial aneurysm; these included SNPs on 2q, 8q and 9p (**Table 1**). At each locus, SNPs in strong LD in the Japanese sample showed highly correlated P values (**Fig. 2**). For associated SNPs, risk alleles in Japan were identical to and showed similar odds ratios to those found in Europe (**Table 1** and **Supplementary Table 3**). Using the Mantel extension test to combine data from all three cohorts, we found the following P values and odds ratios for the SNPs showing the strongest evidence for association at each locus: 2q, $P = 4.4 \times 10^{-8}$ (odds ratio (OR) = 1.24); 8q, $P = 1.4 \times 10^{-10}$ (OR = 1.36); 9p, $P = 1.4 \times 10^{-10}$ (OR = 1.29) (**Table 1**). No locus showed significant deviation from an additive model (log-odds scale) (**Supplementary Table 3**).

We examined the distributions of P values in each significant interval. At 2q, association in Europe lies within a large block of LD (197.8–198.6 Mb; **Fig. 2** and **Supplementary Table 4** online). In Asian subjects, this segment is divided into two smaller blocks of LD and the association seen in Japan is confined to SNPs in the more telomeric block (198.2–198.5 Mb). This interval contains four known genes; the two most strongly associated SNPs, rs700651 and rs700675, lie in introns of adjacent genes, *BOLL* and *PLCL1*. PLCL1 is of interest because it has significant homology to phospholipase C, which lies downstream of VEGFR2 signaling[19]. VEGFR2 is a marker of endothelial progenitor cells and has a role in central nervous system angiogenesis[20].

The LD structure at 8q is also of interest (**Fig. 2** and **Supplementary Table 4**). SNP rs10958409 shows the most significant association; SNPs in high LD with rs10958409 show correlated P values. In addition, however, rs9298506, which lies 110 kb distally and shows virtually no LD with rs10958409 ($r^2 = 0.004$ in European HapMap subjects[21], 0.004 in Finnish cases and 0.0005 in Dutch cases) nonetheless also revealed significant association in Europeans; adjacent SNPs in LD showed correlated P values. This observation suggests the presence of two independent risk alleles. A conditional test of association demonstrated that after accounting for the association with rs9298506, rs10958409 still showed significant association with intracranial aneurysm (and vice versa), consistent with two risk loci (**Supplementary Table 4**). The Japanese cohort replicated association at rs10958409, but not rs9298506, despite having had 88% power to detect association of this latter SNP (**Supplementary Table 3**). Further work will be required to determine whether the European association with rs9298506 is a true positive result. This 8q interval contains a

Table 1 Summary of results for five SNPs that characterize the association with intracranial aneurysm on chromosomes 2, 8 and 9

							Odds ratio (95% CI)						
Chr.	SNP	Pos. (Mb)	Risk allele	Dataset	RAF (control/case)	*P* value[a]	Per allele	Heterozygous	Homozygous	Heterogeneity *P*[b]	Dom. *P*[c]	PAF(%)	RRF(%)
2	rs1429412	197.9	G	Finland	0.42/0.48	4.4×10^{-4}	1.27 (1.11–1.45)	1.33 (1.07–1.65)	1.60 (1.22–2.10)	–	0.60	–	–
				Netherlands	0.34/0.39	1.6×10^{-4}	1.25 (1.11–1.40)	1.35 (1.14–1.61)	1.48 (1.15–1.90)	–	0.21	–	–
				Europe	–	2.5×10^{-7}	1.26 (1.15–1.37)	1.34 (1.18–1.54)	1.54 (1.28–1.85)	0.85	0.21	–	–
				Japan	0.29/0.30	0.42	1.08 (0.90–1.30)	1.05 (0.82–1.35)	1.21 (0.78–1.86)	–	0.76	–	–
				All	–	5.8×10^{-7}	1.22 (1.13–1.32)	1.27 (1.13–1.43)	1.46 (1.24–1.73)	0.32	0.40	–	–
	rs700651	198.3	G	Finland	0.39/0.44	5.6×10^{-3}	1.21 (1.06–1.39)	1.19 (0.96–1.46)	1.48 (1.12–1.96)	–	0.81	14.1	0.7
				Netherlands	0.35/0.40	5.0×10^{-4}	1.23 (1.09–1.38)	1.22 (1.03–1.46)	1.50 (1.18–1.91)	–	0.99	14.1	0.7
				Europe	–	8.9×10^{-6}	1.22 (1.12–1.33)	1.21 (1.06–1.38)	1.49 (1.25–1.79)	0.89	0.87	–	–
				Japan	0.46/0.54	0.0011	1.30 (1.11–1.53)	1.05 (0.79–1.41)	1.70 (1.24–2.33)	–	0.08	14.8	1.6
				All	–	4.4×10^{-8}	1.24 (1.15–1.34)	1.18 (1.04–1.33)	1.56 (1.34–1.83)	0.77	0.30	–	–
8	*rs10958409*	55.5	A	Finland	0.18/0.22	1.4×10^{-3}	1.31 (1.11–1.55)	1.40 (1.15–1.71)	1.34 (0.81–2.21)	–	0.20	11.7	0.9
				Netherlands	0.15/0.20	1.4×10^{-7}	1.46 (1.27–1.68)	1.42 (1.20–1.69)	2.28 (1.51–3.45)	–	0.65	12.1	1.7
				Europe	–	1.6×10^{-9}	1.39 (1.25–1.55)	1.42 (1.25–1.61)	1.83 (1.31–2.55)	0.34	0.64	–	–
				Japan	0.25/0.30	0.016	1.26 (1.04–1.51)	1.21 (0.94–1.55)	1.66 (1.07–2.59)	–	0.66	10.9	0.8
				All	–	1.4×10^{-10}	1.36 (1.24–1.49)	1.37 (1.22–1.54)	1.79 (1.37–2.33)	0.40	0.77	–	–
	rs9298506	55.6	A	Finland	0.73/0.80	4.6×10^{-7}	1.50 (1.28–1.75)	1.26 (0.82–1.94)	1.99 (1.31–3.01)	–	0.41	38.5	2.0
				Netherlands	0.81/0.85	2.3×10^{-4}	1.34 (1.15–1.56)	1.50 (0.87–2.59)	1.97 (1.15–3.35)	–	0.66	–	–
				Europe	–	8.6×10^{-10}	1.41 (1.27–1.58)	1.37 (0.98–1.91)	1.95 (1.41–2.70)	0.32	0.84	–	–
				Japan	0.81/0.83	0.25	1.14 (0.92–1.41)	0.59 (0.30–1.13)	0.78 (0.41–1.47)	–	0.04	–	–
				All	–	1.8×10^{-9}	1.35 (1.22–1.49)	1.16 (0.87–1.56)	1.63 (1.23–2.16)	0.13	0.29	–	–
9	*rs1333040*	22.1	T	Finland	0.47/0.52	2.8×10^{-3}	1.22 (1.07–1.40)	1.23 (0.98–1.54)	1.50 (1.15–1.95)	–	0.96	18.5	0.7
				Netherlands	0.55/0.62	9.5×10^{-7}	1.33 (1.19–1.50)	1.38 (1.09–1.75)	1.80 (1.41–2.31)	–	0.73	30.2	1.4
				Europe	–	1.5×10^{-8}	1.29 (1.18–1.40)	1.30 (1.10–1.53)	1.66 (1.39–1.98)	0.34	0.89	–	–
				Japan	0.65/0.72	0.0024	1.32 (1.10–1.58)	1.26 (0.83–1.91)	1.69 (1.13–2.55)	–	0.81	29.3	1.1
				All	–	1.4×10^{-10}	1.29 (1.19–1.40)	1.29 (1.11–1.50)	1.67 (1.42–1.96)	0.61	1.00	–	–

SNPs that replicate with $P < 0.05$ in the Japanese cohort are italicized. Position shown is from NCBI build 36 coordinates. Risk allele is indexed to the forward strand of NCBI build 36.
[a]The Cochran-Armitage trend test *P* value for cohorts from Finland, Netherlands and Japan, respectively, and the Mantel extension test (uncorrected for λ) *P* value for combined cohorts. [b]*P* value of the test of heterogeneity in effect size among populations. [c]*P* value of the test of deviation from an additive model. PAF, population attributable fraction. RRF, recurrence risk fraction attributable to each SNP, assuming the overall sibling recurrence risk of 4 (ref. 10).

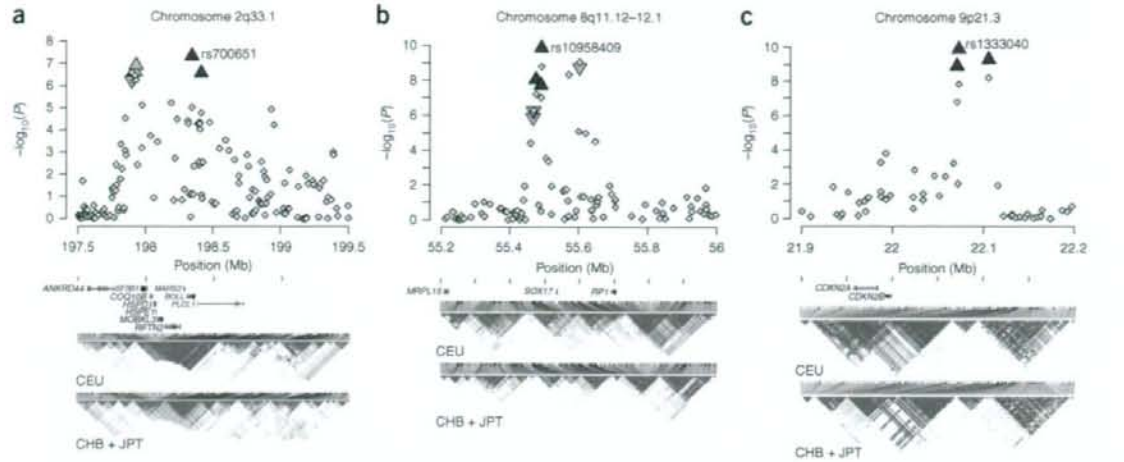

Figure 2 Regional association plots and linkage disequilibrium structure. (**a–c**) The $-\log_{10}$ of the *P* value for association of each SNP and intracranial aneurysm in discovery phase across segments of 2q (**a**), 8q (**b**) and 9q (**c**) are shown as small diamonds (using NCBI build 36 for map locations). Fifteen SNPs that were genotyped in the Japanese replication cohort are shown as triangles that show the combined (discovery + replication) *P* values: blue triangles represent SNPs that demonstrate replication in the Japanese cohort with $P < 0.05$, and gray triangles denote SNPs with $P > 0.05$ in the replication study. SNPs with the most significant *P* values in each interval in the combined analysis are marked with their SNP IDs. Known transcripts (RefSeq database) are represented as horizontal bars at the bottom of each panel. Population-specific LD structures based on D′ are shown for the HapMap European (CEU) and Asian (CHB + JPT) cohorts[21]. The results demonstrate that on chromosome 2, SNPs spanning an ~800-kb interval are in strong LD in the CEU population and show evidence of association with intracranial aneurysm in the Finnish and Dutch cohorts. In Asia, this segment is broken into two smaller blocks of LD that are not strongly correlated with one another, and significant association with intracranial aneurysm in Japanese cohort is seen only for the telomeric segment. For chromosome 8, SNPs in two blocks that are not in significant LD with one another both show significant association with intracranial aneurysm in the European cohort; only SNPs located within the proximal block replicate in Japan. Cohort-specific r^2 values among all SNPs genotyped in the replication studies are shown in **Supplementary Table 4**.

single gene, *SOX17*, which lies between these two association peaks, 43 kb from rs10958409 and 64 kb from rs9298506. The next closest genes lie 201 kb distal and 266 kb proximal to rs10958409. Sox17 has an important role in formation and maintenance of the endothelium (see below).

Finally, SNPs on 9p that showed association with intracranial aneurysm (22.07–22.10 Mb) (**Fig. 2** and **Supplementary Table 4**) were in LD with SNPs that have previously shown association with multiple arterial diseases[2–4]. Adjacent SNPs that are associated with type 2 diabetes mellitus[22–24] showed no significant association with intracranial aneurysm. The strongest association was with rs1333040, which lies 74 kb from the 5′ end of *CDKN2B* and 88 kb from *CDKN2A*. These genes encode the cyclin-dependent kinase inhibitors $p15^{INK4b}$ and $p16^{INK4a}$, as well as ARF, a regulator of p53 activity. In addition, a non-protein-coding transcript (*ANRIL*) lies within this interval[25]. Among these, $p16^{INK4a}$ is of particular interest (see below).

To determine whether the effects of these loci are influenced by known risk factors, we examined the odds ratios of the most significant allele at each locus after partitioning cases by gender, family history of intracranial aneurysm, age (older half versus younger) and ruptured versus unruptured aneurysm. The results showed no significant difference in odds ratios after any of these partitions, suggesting independent contributions to risk (**Supplementary Table 5** online).

Finally, to assess the combined effects of the three loci, we defined each subject's risk score by summing the logarithm of the odds ratio for each risk allele they harbor as determined in each cohort. The observed intracranial aneurysm risk showed a significant linear relationship with risk score in each cohort, with a more than threefold increase from lowest to highest strata (**Table 2** and **Supplementary Table 6** online).

This study provides the first results of a large GWAS of intracranial aneurysm or stroke. Three significant loci have been identified. These results cannot be explained by nonrandom genotyping error or population stratification and are robust to alternative analyses (**Supplementary Fig. 1**). We calculate that these loci collectively account for 38–46% of the population-attributable fraction of intracranial aneurysm and 2.3–3.8% of the sibling recurrence risk (**Table 1**). Additional common variants are likely to have a role in intracranial aneurysm, as the study was not well powered to find loci with GRR <1.25. In addition, population-specific effects were not considered in this study design. Given the risk allele frequencies and odds ratios of the identified loci, future replication cohorts will require ~900 to 1,600 cases and controls to have 80% power for replication ($\alpha = 0.05$).

After genomic control correction and exclusion of SNPs at the four top loci, 37 SNPs remained with *P* values less than 10^{-4} (28 are expected by chance). Some of these may prove to be true risk alleles as additional cohorts are evaluated, as has occurred with type 2 diabetes[26]. In addition, rare variants with larger effects at these same loci may also contribute to the occurrence of intracranial aneurysm[27,28].

Intracranial aneurysms predominate at arterial branch points and sites of shear stress, locations that incur endothelial damage. Vascular injury mobilizes bone marrow–derived cells that localize to these sites and contribute to repair[29,30]. *SOX17*, a member of the Sry-related HMG box transcription factor family, is of particular interest because it is required for both endothelial formation and maintenance[6–8]. Sox17 plays a key role in the generation and maintenance of fetal and neonatal stem cells of both hematopoietic and endothelial lineages[8] and is expressed in adult endothelium[6]. $Sox17^{-/-}$ mice show multiple vascular abnormalities[7]; moreover, whereas $Sox18^{-/-}$ mice are normal, $Sox18^{-/-}$;$Sox17^{+/-}$ mice show defective endothelial sprouting and

Table 2 Increased intracranial aneurysm risk with increased risk score based on genotypes for rs700651, rs10958409 and rs133040

	Japan			Netherlands			Finland		
No. of risk alleles	Frequency (control/case)	Average risk score (min–max)	OR (95% CI)	Frequency (control/case)	Average risk score (min–max)	OR (95% CI)	Frequency (control/case)	Average risk score (min–max)	OR (95% CI)
0 or 1	0.14/0.08	0.23 (0.00–0.28)	1	0.3/0.21	0.22 (0.00–0.38)	1	0.32/0.21	0.17 (0.00–0.27)	1
2	0.28/0.21	0.53 (0.46–0.55)	1.29 (0.81–2.05)	0.36/0.29	0.54 (0.41–0.75)	1.13 (0.9–1.41)	0.34/0.34	0.42 (0.38–0.54)	1.47 (1.15–1.88)
3	0.33/0.32	0.79 (0.72–0.82)	1.63 (1.05–2.55)	0.25/0.33	0.82 (0.70–1.04)	1.88 (1.51–2.34)	0.24/0.3	0.63 (0.59–0.74)	1.82 (1.41–2.36)
4	0.19/0.28	1.05 (0.99–1.08)	2.41 (1.51–3.83)	0.08/0.14	1.10 (0.98–1.33)	2.40 (1.82–3.16)	0.07/0.13	0.85 (0.79–0.94)	2.83 (1.98–4.04)
5 or 6	0.06/0.10	1.34 (1.26–1.54)	2.91 (1.62–5.21)	0.02/0.03	1.41 (1.36–1.74)	2.63 (1.56–4.41)	0.03/0.02	1.09 (1.06–1.33)	1.16 (0.62–2.19)
P value[a]		3.3×10^{-7}			8.4×10^{-16}			7.8×10^{-8}	
OR (95% CI)[b]		2.91 (1.92–4.41)			2.81 (2.19–3.61)			2.88 (1.95–4.25)	

Individuals with non-missing genotypes for all six alleles were included in the analysis.
[a]*P* value for linear relationship of risk score and logarithm of ORs (complete data set is listed in **Supplementary Table 6**). [b]Increase in odds ratio per one unit change in risk score.

vascular remodeling[6]. Similarly, $p16^{INK4a}$ has a role in regulation of stem (progenitor) cell populations, including bone marrow–derived cells of the vasculature[9]. These considerations suggest that intracranial aneurysm may result from defective stem (progenitor) cell–mediated vascular development and/or repair.

Finally, these findings have implications for identification of individuals with intracranial aneurysm before morbid events. The odds ratio of intracranial aneurysm increases greater than threefold in subjects with the highest versus the lowest risk (**Table 2** and **Supplementary Table 6**). Although we caution that further work is required, these findings advance the potential for preclinical diagnosis by combined assessment of inherited susceptibility with previously established risk factors.

METHODS

Cohorts. The study protocol was approved by the Yale Human Investigation Committee (HIC protocol 7680). In all cases, the diagnosis of intracranial aneurysm was made with computerized tomography angiogram, magnetic resonance angiogram or cerebral digital subtraction angiogram and confirmed at surgery, when applicable. Rupture of aneurysm was defined by identification of acute subarachnoid hemorrhage (via computerized tomography or magnetic resonance imaging) from a proven aneurysm. Cases with a first-degree relative with intracranial aneurysm were considered familial, and other cases were considered sporadic.

Three cohorts from independent studies in Finland, The Netherlands and Japan were collected and all participants provided informed consent. There were 960 Finnish cases and 1,017 controls; 786 Dutch cases and 6,424 controls; and 495 Japanese cases and 676 controls. Japanese controls were screened for not harboring intracranial aneurysm.

Genotyping and SNP quality control. Genome-wide genotyping in European cohorts was done on the Illumina platform according to the manufacturer's protocol (Illumina). We genotyped subjects on either the CNV370-Duo, HumanHap300 or HumanHap550 chips. SNPs shared across all platforms ($n = 314{,}125$) were extracted. We applied prespecified criteria to exclude samples and SNPs that performed poorly as well as samples that could not be genetically well matched (**Supplementary Table 1** and **Supplementary Methods**). The overall median genotype call rate was 99.7% and the mean heterozygosity of all SNPs was 35%. Seventy-two duplicate pairs of samples were genotyped and showed 99.91% genotype identity. We carried out detailed analysis of the performance of SNPs across cohorts and platforms to ensure that significant associations observed were not due to differences in SNP performance (**Supplementary Table 2**).

Cryptic relatedness. We determined the identity by state (IBS) similarity and estimated the degree of relatedness for each pair of samples in the GWAS (**Supplementary Methods**) and excluded inferred first- and second-degree relatives (**Supplementary Table 1**).

Analysis of population structure. In order to identify population outliers and cases whose genetic ancestry cannot be properly matched to controls (and vice versa), we used the Genetic Matching (GEM) method described previously[16] based on principal component analysis (PCA). After this matching process, three significant principal components remained in the Finnish cohort and none in the Dutch cohort, as previously observed (**Supplementary Methods**).

After quality control and analysis of population structure, there remained 874 cases and 944 controls in the Finnish cohort and 706 cases and 5,332 controls in the Dutch cohort. Among the Finnish cases, 57% were female; 73% had suffered ruptured aneurysm and 43% had positive family history; the median age at diagnosis was 50 years (those with rupture 49 years versus those without rupture 52 years). In the Dutch cohort, 69% were female, 92% had ruptured aneurysm, 15% had a positive family history and the median age was 49 years.

SNP association analysis. To test for association of each SNP with intracranial aneurysm, we assumed an additive (in log-odds scale) model. We used the Cochran-Armitage trend test for each cohort. For the combined sample of European descent or of European and Japanese cohorts, we used the Mantel extension test (**Supplementary Methods**).

We calculated the per-allele and genotype-specific ORs and their 95% confidence intervals by fitting 1-d.f. and 2-d.f. logistic models, respectively. We assessed heterogeneity of ORs among populations by considering the likelihood ratios of a logistic model with population by genotype interaction term(s) versus a linear model without the interaction term(s) and used a *P* value <0.05 as evidence of significant heterogeneity (**Supplementary Table 3**). To evaluate the degree of overdispersion of test statistics, we calculated the genomic inflation factor (λ) for each statistical test by the ratio of the mean of the lower 90% of observed test statistics to that of the expected χ^2 values[17]. We applied the genomic control method to correct for λ (**Fig. 1b**) and then compared a pairwise plot of *P* values for each SNP in the trend and corrected tests to determine the potential effect of any residual population stratification (**Supplementary Fig. 1a,b** and **Supplementary Methods**).

We also examined the validity of the assumption of additivity (in log-odds scale) in the association tests by comparing likelihood ratios assuming

alternative models of dominance and rejected additivity for $P < 0.05$ (ref. 2 and **Supplementary Table 3**).

For each chromosome segment showing significant association with intracranial aneurysm, we investigated whether more than one SNP had an independent marginal effect on intracranial aneurysm by the Mantel extension test conditioned on genotypes for SNPs within each interval (**Supplementary Table 4**).

To assess the robustness of our GWAS results, we also performed a weighted *Z*-score test and found that the results of this alternative analysis were highly correlated with the results of the Mantel extension test (**Supplementary Fig. 1c**).

Replication study in Japanese cohort. For the Japanese replication study, allelic discrimination assays were done with 15 SNPs on the Sequenom iPLEX genotyping platform according to the manufacturer's protocol. For SNPs that showed significant *P* values, genotypes were repeated and *P* values confirmed on the TaqMan platform (Applied Biosystems). Association tests were done as described above, using $P = 0.05$ (in the Cochran-Armitage trend test with the same allele found associated in Europe) as the threshold for significance (**Supplementary Table 3**).

Subset analysis. For SNPs with the most significant *P* values we investigated whether the association results were affected by potential confounding variables such as rupture status, family history or gender. We compared genotype distributions of cases stratified by these variables using the trend test (**Supplementary Table 5**).

Population-attributable fraction and proportion of genetic variance attributable to SNPs. We investigated two risk measures based on replicated SNPs: the population attributable fraction (PAF) and the proportion of the sibling recurrence risk attributable to a SNP ('recurrence risk fraction') as previously described (**Table 1** and **Supplementary Methods**). For these calculations we assumed intracranial aneurysm population prevalence of 2% and λ_{sib} of 4 (ref. 10). The combined contribution of SNPs was obtained by assuming the multiplicative model (**Supplementary Methods**).

Cumulative effects of risk alleles. We analyzed the cumulative effects of the risk alleles at the most significant SNP at 2q, 8q and 9p (rs700651, rs10958409 and rs1333040) by calculating the risk score for each individual by the weighted sum of the number of risk alleles as defined by

$$\text{Risk score} = \sum_i \psi[i]n[i]$$

where $\psi[i]$ is the logarithm of the calculated per-allele odds ratio at each locus and $n[i]$ is the number of risk alleles at the same locus. We then assessed the risk score for each of the 27 possible three-locus genotypes in each cohort (**Supplementary Table 6**). We fitted a simple linear logistic model with an additive effect (on log-odds scale) for each cohort and performed a likelihood-ratio test. For display purposes, the 27 strata of **Supplementary Table 6** are compressed into 5 strata shown in **Table 2** according to the absolute number of risk alleles, which closely parallels the risk score.

Note: Supplementary information is available on the Nature Genetics website.

ACKNOWLEDGMENTS

We are grateful to the participants who made this study possible. We thank A. Chamberlain, O. Törnwall, M. Alalahti, K. Helin, S. Malin and J. Budzinack for their technical help. This study was supported by the Yale Center for Human Genetics and Genomics and the Yale Program on Neurogenetics, the US National Institutes of Health grants R01NS057756 (M.G.) and U24 NS051869 (S.M.) and the Howard Hughes Medical Institute (R.P.L.). C.E.M. and M.W.S. are supported by a gift from the Lawrence Family and Y.M.R. by the Dr E. Dekker program of The Netherlands Heart Foundation (2005T014). K.Y. and I.I. were supported by the Core Research for Evolutional Science and Technology, Japan Science and Technology Corporation.

AUTHOR CONTRIBUTIONS

Cohort ascertainment, characterization and DNA preparation: M.N., E.G., A.L., A.P., J.Ö. and J.H. (Helsinki); M.v.u.z.F., A.R., T.K., J.R., A.P. and J.E.J. (Kuopio); Y.M.R., L.H.v.d.B., C.W. and G.J.E.R. (Utrecht); C.M.v.D. and M.M.B.B. (Rotterdam) and A.T., A.H., H.K. and I.I. (Japan). Genotyping: K.B., Y.B., L.K., Z.A., S.R., R.P.L., M.G. and S.M. Study design and analysis plan: R.P.L. and M.G. Data management and informatics: C.E.M., K.B., M.W.S. and M.G. Statistical analysis: K.Y., K.B., I.I., M.C., R.P.L. and M.G. Writing team: K.B., K.Y., M.W.S., M.G. and R.P.L.

Published online at http://www.nature.com/naturegenetics/
Reprints and permissions information is available online at http://npg.nature.com/reprintsandpermissions/

1. Bederson, J.B. *et al.* Recommendations for the management of patients with unruptured intracranial aneurysms: a Statement for healthcare professionals from the Stroke Council of the American Heart Association. *Stroke* **31**, 2742–2750 (2000).
2. Wellcome Trust Case Control Consortium. Genome-wide association study of 14,000 cases of seven common diseases and 3,000 shared controls. *Nature* **447**, 661–678 (2007).
3. McPherson, R. *et al.* A common allele on chromosome 9 associated with coronary heart disease. *Science* **316**, 1488–1491 (2007).
4. Helgadottir, A. *et al.* A common variant on chromosome 9p21 affects the risk of myocardial infarction. *Science* **316**, 1491–1493 (2007).
5. Helgadottir, A. *et al.* The same sequence variant on 9p21 associates with myocardial infarction, abdominal aortic aneurysm and intracranial aneurysm. *Nat. Genet.* **40**, 217–224 (2008).
6. Matsui, T. *et al.* Redundant roles of Sox17 and Sox18 in postnatal angiogenesis in mice. *J. Cell Sci.* **119**, 3513–3526 (2006).
7. Sakamoto, Y. *et al.* Redundant roles of Sox17 and Sox18 in early cardiovascular development of mouse embryos. *Biochem. Biophys. Res. Commun.* **360**, 539–544 (2007).
8. Kim, I., Saunders, T.L. & Morrison, S.J. Sox17 dependence distinguishes the transcriptional regulation of fetal from adult hematopoietic stem cells. *Cell* **130**, 470–483 (2007).
9. Janzen, V. *et al.* Stem-cell ageing modified by the cyclin-dependent kinase inhibitor p16INK4a. *Nature* **443**, 421–426 (2006).
10. Schievink, W.I., Schaid, D.J., Michels, V.V. & Piepgras, D.G. Familial aneurysmal subarachnoid hemorrhage: a community-based study. *J. Neurosurg.* **83**, 426–429 (1995).
11. Foroud, T. *et al.* Genome screen to detect linkage to intracranial aneurysm susceptibility genes: the Familial Intracranial Aneurysm (FIA) study. *Stroke* **39**, 1434–1440 (2008).
12. Nahed, B.V. *et al.* Mapping a mendelian form of intracranial aneurysm to 1p34.3-p36.13. *Am. J. Hum. Genet.* **76**, 172–179 (2005).
13. Ozturk, A.K. *et al.* Molecular genetic analysis of two large kindreds with intracranial aneurysms demonstrates linkage to 11q24–25 and 14q23–31. *Stroke* **37**, 1021–1027 (2006).
14. Ruigrok, Y.M. *et al.* Genomewide linkage in a large Dutch family with intracranial aneurysms: replication of 2 loci for intracranial aneurysms to chromosome 1p36.11-p36.13 and Xp22.2-p22.32. *Stroke* **39**, 1096–1102 (2008).
15. Gudbjartsson, D.F. *et al.* Variants conferring risk of atrial fibrillation on chromosome 4q25. *Nature* **448**, 353–357 (2007).
16. Luca, D. *et al.* On the use of general control samples for genome-wide association studies: genetic matching highlights causal variants. *Am. J. Hum. Genet.* **82**, 453–463 (2008).
17. Clayton, D.G. *et al.* Population structure, differential bias and genomic control in a large-scale, case-control association study. *Nat. Genet.* **37**, 1243–1246 (2005).
18. Freedman, M.L. *et al.* Assessing the impact of population stratification on genetic association studies. *Nat. Genet.* **36**, 388–393 (2004).
19. Shibuya, M. Differential roles of vascular endothelial growth factor receptor-1 and receptor-2 in angiogenesis. *J. Biochem. Mol. Biol.* **39**, 469–478 (2006).
20. Ziegler, B.L. *et al.* KDR receptor: a key marker defining hematopoietic stem cells. *Science* **285**, 1553–1558 (1999).
21. Frazer, K.A. *et al.* A second generation human haplotype map of over 3.1 million SNPs. *Nature* **449**, 851–861 (2007).
22. Zeggini, E. *et al.* Replication of genome-wide association signals in UK samples reveals risk loci for type 2 diabetes. *Science* **316**, 1336–1341 (2007).
23. Scott, L.J. *et al.* A genome-wide association study of type 2 diabetes in Finns detects multiple susceptibility variants. *Science* **316**, 1341–1345 (2007).
24. Saxena, R. *et al.* Genome-wide association analysis identifies loci for type 2 diabetes and triglyceride levels. *Science* **316**, 1331–1336 (2007).
25. Pasmant, E. *et al.* Characterization of a germ-line deletion, including the entire INK4/ARF locus, in a melanoma-neural system tumor family: identification of ANRIL, an antisense noncoding RNA whose expression coclusters with ARF. *Cancer Res.* **67**, 3963–3969 (2007).
26. Zeggini, E. *et al.* Meta-analysis of genome-wide association data and large-scale replication identifies additional susceptibility loci for type 2 diabetes. *Nat. Genet.* **40**, 638–645 (2008).
27. Romeo, S. *et al.* Population-based resequencing of ANGPTL4 uncovers variations that reduce triglycerides and increase HDL. *Nat. Genet.* **39**, 513–516 (2007).
28. Ji, W. *et al.* Rare independent mutations in renal salt handling genes contribute to blood pressure variation. *Nat. Genet.* **40**, 592–599 (2008).
29. Asahara, T. *et al.* Isolation of putative progenitor endothelial cells for angiogenesis. *Science* **275**, 964–967 (1997).
30. Purhonen, S. *et al.* Bone marrow-derived circulating endothelial precursors do not contribute to vascular endothelium and are not needed for tumor growth. *Proc. Natl. Acad. Sci. USA* **105**, 6620–6625 (2008).

Genome-Wide Expression of Azoospermia Testes Demonstrates a Specific Profile and Implicates *ART3* in Genetic Susceptibility

Hiroyuki Okada[1☯], Atsushi Tajima[2☯], Kazuyoshi Shichiri[3], Atsushi Tanaka[4], Kenichi Tanaka[1], Iturо Inoue[2,5*]

1 Department of Obstetrics and Gynecology, Niigata University Graduate School of Medical and Dental Sciences, Niigata, Japan, **2** Division of Molecular Life Science, School of Medicine, Tokai University, Isehara, Japan, **3** Department of Obstetrics and Gynecology, Tachikawa Hospital, Nagaoka, Japan, **4** St. Mother's Hospital, Kitakyushu, Japan, **5** Core Research for Evolutional Science and Technology, Japan Science and Technology Corporation, Kawaguchi, Japan

Infertility affects about one in six couples attempting pregnancy, with the man responsible in approximately half of the cases. Because the pathophysiology underlying azoospermia is not elucidated, most male infertility is diagnosed as idiopathic. Genome-wide gene expression analyses with microarray on testis specimens from 47 non-obstructive azoospermia (NOA) and 11 obstructive azoospermia (OA) patients were performed, and 2,611 transcripts that preferentially included genes relevant to gametogenesis and reproduction according to Gene Ontology classification were found to be differentially expressed. Using a set of 945 of the 2,611 transcripts without missing data, NOA was further categorized into three classes using the non-negative matrix factorization method. Two of the three subclasses were different from the OA group in Johnsen's score, FSH level, and/or LH level, while there were no significant differences between the other subclass and the OA group. In addition, the 52 genes showing high statistical difference between NOA subclasses ($p < 0.01$ with Tukey's *post hoc* test) were subjected to allelic association analyses to identify genetic susceptibilities. After two rounds of screening, SNPs of the ADP-ribosyltransferase 3 gene (*ART3*) were associated with NOA with highest significance with ART3-SNP25 (rs6836703; $p = 0.0025$) in 442 NOA patients and 475 fertile men. Haplotypes with five SNPs were constructed, and the most common haplotype was found to be under-represented in patients (NOA 26.6% versus control 35.3%, $p = 0.000073$). Individuals having the most common haplotype showed an elevated level of testosterone, suggesting a protective effect of the haplotype on spermatogenesis. Thus, genome-wide gene expression analyses were used to identify genes involved in the pathogenesis of NOA, and *ART3* was subsequently identified as a susceptibility gene for NOA. These findings clarify the molecular pathophysiology of NOA and suggest a novel therapeutic target in the treatment of NOA.

Citation: Okada H, Tajima A, Shichiri K, Tanaka A, Tanaka K, et al. (2008) Genome-wide expression of azoospermia testes demonstrates a specific profile and implicates ART3 in genetic susceptibility. PLoS Genet 4(2) e26. doi:10.1371/journal.pgen.0040026

Introduction

Spermatogenesis, a major function of mammalian testes, is complex and strictly regulated. While spermatogenesis is a maturation of germ cells, other cells including Sertoli, Leydig, and peritubular myoid cells also play important roles, and defects at any differentiation stage might result in infertility. Male infertility is estimated to affect about 5% of adult human males, but 75% of the cases are diagnosed as idiopathic because the molecular mechanisms underlying the defects have not been elucidated. In consequence, an estimated one in six couples experiences difficulty in conceiving a child despite advances in assisted reproductive technologies. Male-factor infertility constitutes about half of the cases, and a significant proportion of male infertility is accompanied by idiopathic azoospermia or severe oligozoospermia, which may well have potential genetic components. It is well-recognized that men with very low sperm counts (<1 million/ml), identified through an infertility clinic, have a higher incidence of Y-chromosome microdeletion (up to 17%) [1,2]. However, the genetic causalities of most cases of azoospermia are not known.

Global gene-expression profiling with microarray technologies has been applied with great promise to monitor biological phenomena and answer biological questions. Indeed, microarray technologies have been successfully used to identify biomarkers, disease subtypes, and mechanisms of toxicity. We applied microarray analysis to testis specimens from infertile individuals including patients with obstructive azoospermia (OA) and non-obstructive azoospermia (NOA [OMIM %606766]) to characterize NOA and to identify the specific pathophysiology and molecular pathways of the disease. In addition, we attempted to identify genetic susceptibility to NOA from genes differentially expressed in NOA testes.

Editor: Emmanouil T. Dermitzakis, The Wellcome Trust Sanger Institute, United Kingdom

Received July 31, 2007; **Accepted** December 13, 2007; **Published** February 8, 2008

Abbreviations: ART3, ADP-ribosyltransferase 3; AZF, azoospermia factor; coph, cophenetic correlation coefficient; Cy3, cyanine 3-CTP; Cy5, cyanine 5-CTP; EM, expectation–maximization; FDR, false discovery rate; FSH, follicle-stimulating hormone; GO, Gene Ontology; HC, hierarchical clustering; LD, linkage disequilibrium; LH, leutenizing hormone; MAF, minor allele frequency; MESA, microsurgical epididymal sperm aspiration; NMF, non-negative matrix factorization; NOA, non-obstructive azoospermia; OA, obstructive azoospermia; R^2, square of correlation coefficient; SNP, single nucleotide polymorphism; TESE, testicular sperm extraction

* To whom correspondence should be addressed. E-mail: ituro@is.icc.u-tokai.ac.jp

☯ These authors contributed equally to this work.

Author Summary

Worldwide, approximately 15% of couples attempting pregnancy meet with failure. Male factors are thought to be responsible in 20%–50% of all infertility cases. Azoospermia, the absence of sperm in the ejaculate due to defects in its production or delivery is common in male infertility. In this study, we focused on non-obstructive azoospermia (NOA) because the etiologies of obstructive azoospermia are well studied and distinct from those of NOA. Microdeletions of the Y chromosome are thus far the only genetic defects known to affect human spermatogenesis, but most cases of NOA are unsolved. Because NOA results from a variety of defects in the developmental stages of spermatogenesis, the stage-specific expressions of genes in the testes must be investigated. Thus, genome-wide gene expression analyses of testes of NOA can provide insight into the several etiologies and genetic susceptibilities of NOA. In the present study, we analyzed several differentially expressed genes in NOA subclasses and identified ART3 as a susceptibility gene for NOA.

Genes related to spermatogenesis and candidate genes for azoospermia have been surveyed in humans and mice, especially since gene targeting technology accelerated the identification of genes that play crucial roles in spermatogenesis [3]. Because spermatogenesis is a complex process including meiosis, a germ cell–specific event, gene expression profiles specific to the differentiation stage, clinically classified by the Johnsen's score, were examined to provide insight into the pathogenesis of azoospermia [4]. In the current study, we performed microarray analyses on biopsied testes obtained from 47 NOA patients at diverse clinical stages without prior selection and 11 OA patients. The 47 NOA samples showed a wide range of heterogeneity, including a series of impairments at the differentiation stage of spermatogenesis that so far have been evaluated mainly by pathological findings. Thus, classification of NOA at the transcriptome level is a necessary first step in elucidation of the molecular pathogenesis of NOA. To do this, we adopted the non-negative matrix factorization (NMF) method, an unsupervised classification algorithm developed for decomposing images that has been applied in various fields of science including bioinformatics because of its potential for providing insight into complex relationships in large data sets [5–7]. 47 of the NOA-samples were divided into three subclasses by the NMF method, and each class was associated with clinical features. 149 transcripts were identified as differentially expressed genes among the NOA subclasses according to a statistical criterion, and the features involved in spermatogenesis based on Gene Ontology classification were demonstrated.

The genetic causality of NOA most likely involves the expression level of a susceptibility gene, which might be detected by genome-wide gene expression analysis. While it is daunting to identify genetic susceptibility from 100-1000 differentially expressed genes, genetic susceptibility might more readily be identified from random genes differentially expressed with high significance rather than by investigating only genes in a specific biological pathway. Based on a well-defined statistical procedure, 52 candidate genes for NOA were catalogued by gene expression profile and screened for allelic association study in a total of 442 NOA patients and 475 fertile male controls. After gene-centric selection of SNPs, 191 SNPs of 42 candidate genes were initially evaluated for allelic association with NOA. After two rounds of screening, SNPs of the ADP-ribosyltransferase 3 (*ART3*) gene were found to be significantly associated with NOA, and five of these SNPs were selected for haplotype construction. The most common haplotype was significantly under-represented in the patients and may be protective. The functional impact of this haplotype was further investigated.

Results

Extraction of NOA-Related Gene Expression Profile

As shown in Figure 1A, the most notable difference in histological findings between NOA and OA testes was that the NOA patients exhibited, at varying degrees, incomplete sets of spermatogenic germ cells (spermatogonia, spermatocytes, spermatids, and spermatozoa) in the seminiferous tubules. In severe NOA patients, we could not even detect Sertoli cells, the major somatic cells of the seminiferous tubules, on histological examination (figure not shown), indicating clinical heterogeneity of NOA testes. In order to elucidate the molecular systems underlying NOA at the transcriptome level, it is important to extract genes reflecting the diversity of NOA phenotypes. For this purpose, we first compared global gene expression profiles in NOA testes to those of OA testes using the Agilent Human 1A(v2) Oligo Microarray system. We chose the 'standard reference design' in two-color microarray experiments as an experimental design for the expression analysis [8], where a single microarray was used to compare either NOA or OA to the testicular reference RNA as described in Materials and Methods (Figure 1B).

Of the 18,716 transcripts screened with the microarray, we obtained transcripts that showed a 2-fold mean expression difference between NOA and the reference, the NOA group; the OA group comprised transcripts showing less than 2-fold mean expression difference between OA and the reference (Figure 1B). Of the transcripts overlapping the two groups, 2,611 transcripts were found to be differentially expressed between NOA and OA testes after statistical filtering (based on lowess-normalized natural log[Cy5/Cy3], Bonferroni's corrected $p < 0.05$). This gene list, termed NOA-related target genes, comprised 902 elevated and 1,709 decreased transcripts in NOA testes. To characterize the gene list from the biological aspect, the 2,611 transcripts were subjected to functional clustering according to Gene Ontology (GO) classification for biological processes with GeneSpring software. We identified a total of 190 GO categories that were significantly ($p < 0.05$ without multiple testing correction) over-represented among the 2,611 transcripts. Table 1 shows the ten top-ranked GO categories in descending order of significance based on p-values with Fisher's exact test. It is notable that the GO categories involved in gametogenesis (GO:48232; 7283; 7276), reproduction (GO:19953; 3), and the cell cycle (GO:279; 51301; 7049; 7067) are significantly associated with the gene list. We further analyzed two separate subsets comprising 1,709 decreased (Figure 2, upper) and 902 elevated (Figure 2, lower) transcripts, based on their GO annotations. The top-ranked GO categories for NOA-related target genes are more similar to those of the 1,709 decreased transcripts than to those of the 902 elevated ones (Figure 2; Table 1). Thus, the predominant features may reflect spermatogenic defects common to NOA testes. On the

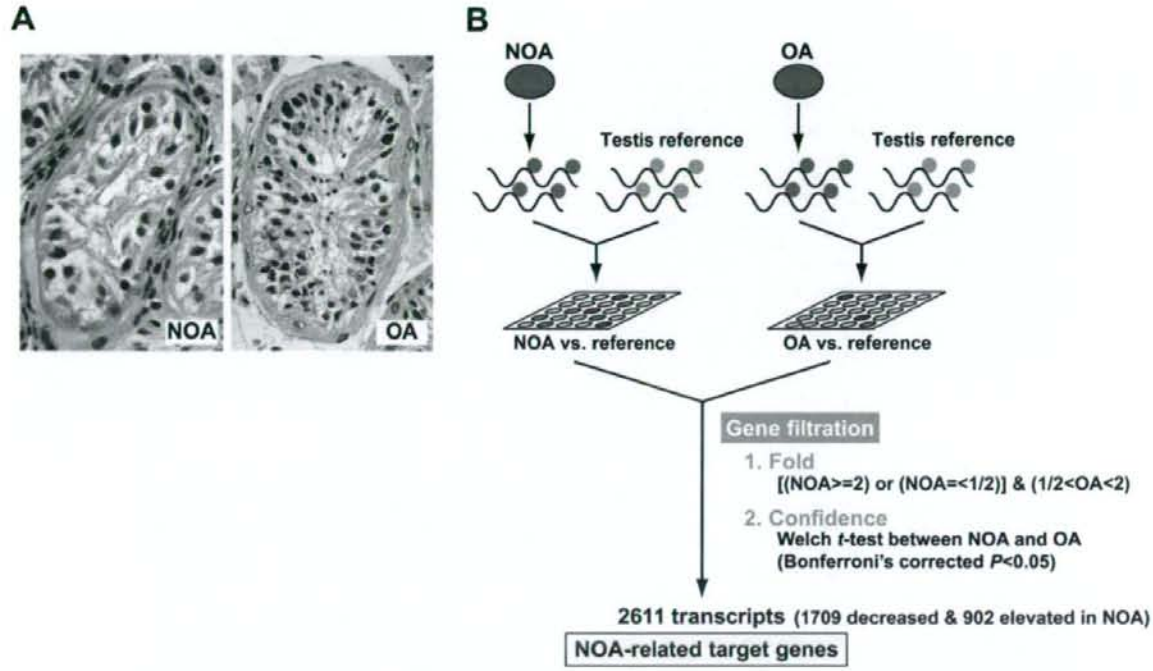

Figure 1. Experimental Design to Extract NOA-related Target Genes

(A) Representative testicular biopsies from NOA (left panel) and OA (right panel) patients. The seminiferous tubules in NOA testis show Sertoli cells only; testicular histology of the OA patient indicates the presence of germ cells at all stages of spermatogenesis.

(B) Strategy for discovering the NOA-specific expression profile, i.e., the NOA-related target genes. Compared with the expression level of reference RNA, the NOA group, with expression undergoing 2-fold or more mean change, was extracted; the OA group comprised transcripts with less than 2-fold mean expression change. Of the overlapping transcripts, only those with statistically significant difference between NOA and OA ($p < 0.05$ with Bonferroni's correction) were identified as differentially expressed.

doi:10.1371/journal.pgen.0040026.g001

Table 1. Top-Ranked Ten Categories of Gene Ontology Significantly Overrepresented among 2,611 Transcripts

GO Category[a]	Genes within GO Category		−logP[c]
	Number	Percent[b]	
Male gamete generation (GO:48232)	55	3.1	12.0
Spermatogenesis (GO:7283)	55	3.1	12.0
Sexual reproduction (GO:19953)	70	3.9	11.2
Gametogenesis (GO:7276)	59	3.3	10.5
Reproduction (GO:3)	75	4.2	8.3
M phase (GO:279)	57	3.2	6.7
Microtubule-based process (GO:7017)	42	2.4	6.5
Cell division (GO:51301)	48	2.7	6.5
Cell cycle (GO:7049)	144	8.1	6.4
Mitosis (GO:7067)	45	2.5	5.6

[a]All GO categories are from the subontology *biological process*.

[b]Percent denotes the percentage of coverage of NOA-related target genes. Of the 2,611 transcripts in the gene list, 1,784 are used for calculating the percentage of genes with a given GO annotation because the GO annotations regarding *biological process* for the others are not available.

[c]*p*-Value was determined by Fisher's exact test, comparing the observed percentage of NOA-related target genes with a given GO annotation to that of genes on the Agilent Human 1A(v2) microarray with the same GO annotation.

doi:10.1371/journal.pgen.0040026.t001

other hand, 902 transcripts elevated in NOA testes exhibited a distinct GO profile that included several GO categories involved in biosynthesis and metabolism in cytoplasm (Figure 2), implying an increase in cytoplasmic turnover rates such as steroid turnover in NOA testes.

Discovery of Three Molecular Subclasses of NOA Testes

To clarify heterogeneity of NOA testes at the transcriptome level, we further examined NOA-related target genes to identify NOA subclasses without prior classification with pathological features. We adopted the NMF algorithm coupled with a model selection method [6] to a complete dataset of 945 out of the 2,611 transcripts without missing values of signal intensities for a total of 47 NOA samples. Figure 3A shows reordered consensus matrices averaging 50 connective matrices generated for subclasses $K = 2$, 3, 4, and 5. Distinct patterns of block partitioning were observed at models with 2 and 3 subclasses ($K = 2$ and 3), whereas higher ranks ($K = 4$ and 5) made block partitioning indistinct. Thus, the NMF method predicts the existence of reproducible and robust subclasses of NOA samples for $K = 2$ and 3. This prediction was quantitatively supported by higher values of cophenetic correlation coefficients (coph) for NMF-clustered matrices. The NMF class assignment for $K = 3$ showed the highest coph value (coph = 0.993), indicating that three molecular subclasses, termed NOA1, NOA2, and NOA3, are

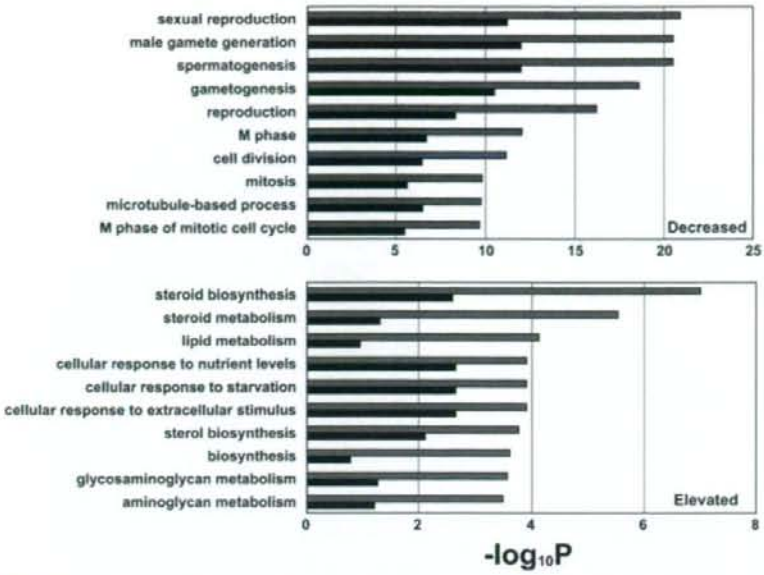

Figure 2. Comparison of Ten Top-ranked Gene Ontology (GO) Categories Significantly Over-Represented in the Two Subsets (1,709 Decreased, Upper Panel; 903 Elevated, Lower Panel) of NOA-related Target Genes

Blue and red bars represent *p*-values for the ten top-ranked GO categories over-represented in the decreased and elevated gene lists, respectively. Black bars show the corresponding *p*-value using 2,611 NOA-related target genes. *p*-Values were determined by Fisher's exact test using all of the GO-annotated genes on the Agilent Human 1A(v2) microarray as a background, as shown in Table 1. The *p*-values are expressed as the negative logarithm (base 10).

doi:10.1371/journal.pgen.0040026.g002

the most reasonable subclassification among 47 NOA samples. For comparative analysis of class discovery, a hierarchical clustering (HC) approach was applied to log-transformed normalized ratios for NOA-related target genes. As shown in Figure 3B, the HC dendrogram exhibited a clustering pattern similar to that of the NMF-based subclassification, as the three NMF-subclasses of NOA samples tended to form distinct clusters in the HC analysis. Thus, the HC clustering for NOA-related target genes appears to justify the three NMF-based subclasses of NOA samples.

To investigate the clinical features of the three NOA subclasses, we compared several clinical measures among the subclasses. The results obtained from statistical analyses in a total of four groups including the OA group are summarized in Table 2. We found significant differences in the three NOA-related clinical characteristics, testicular histological score (Johnsen's score, $p = 1.4 \times 10^{-6}$), serum FSH level ($p = 9.8 \times 10^{-4}$), and LH level ($p = 0.0051$) among the four groups using Kruskal-Wallis test, but there were no differences in age and serum testosterone level. *Post hoc* pairwise comparisons revealed that both the NOA1 and NOA2 groups exhibited low Johnsen's scores and high levels of serum FSH compared with the OA group (Table 2). In the NOA1 group, a high LH level ($p < 0.01$) also was found compared with the OA group. On the other hand, there were no significant differences in any of the parameters between the NOA3 and OA groups, as well as among three NOA subclasses in *post hoc* analysis. Elevations of serum FSH and LH concentrations often are observed in infertile patients with abnormal testicular histologies and are correlated, to some extent, with the severity of spermatogenic defects [9,10]. Testicular histologies of NOA and OA patients have been evaluated by the Johnsen's scores, ranging from 10 to 1 according to the presence or absence of spermatogenesis-related cell types (spermatozoa, spermatids, spermatocytes, spermatogonia, and Sertoli cells) in seminiferous tubules [11]. The NMF-based subclasses of testicular gene expression showed that the low score classes had heterogeneity (NOA1 and NOA2), presumably indicating the possibility of distinct spermatogenic defects at the molecular level that could not be detected by morphological examination.

Identification of Transcripts Differentially Expressed in the Three NOA Subclasses

Based on the three NOA subclasses, we conducted further statistical analyses to extract transcripts representing expression differences between NOA subclasses from the NOA-related target genes (Figure S1). 149 out of 2,611 transcripts showed significant differences ($p < 0.05$, Tukey's *post hoc* test) in testicular expression between the NOA subclasses, as summarized in Table S1. To characterize this gene list based on GO classification for biological processes, we examined which GO terms were highly associated with the 149 differentially expressed transcripts, relative to those for the NOA-related gene list (as shown in Table 1 and Figure 2). Figure 4 shows the 10 top-ranked GO categories for the 149 transcripts, using the 2,611 NOA-related target transcripts as a background set of genes for this GO analysis. Nine GO categories excluding gametogenesis appeared to be novel, indicating that highly significant enrichments of transcripts involved in DNA metabolism (GO:6259; 6325; 6323; 6281),

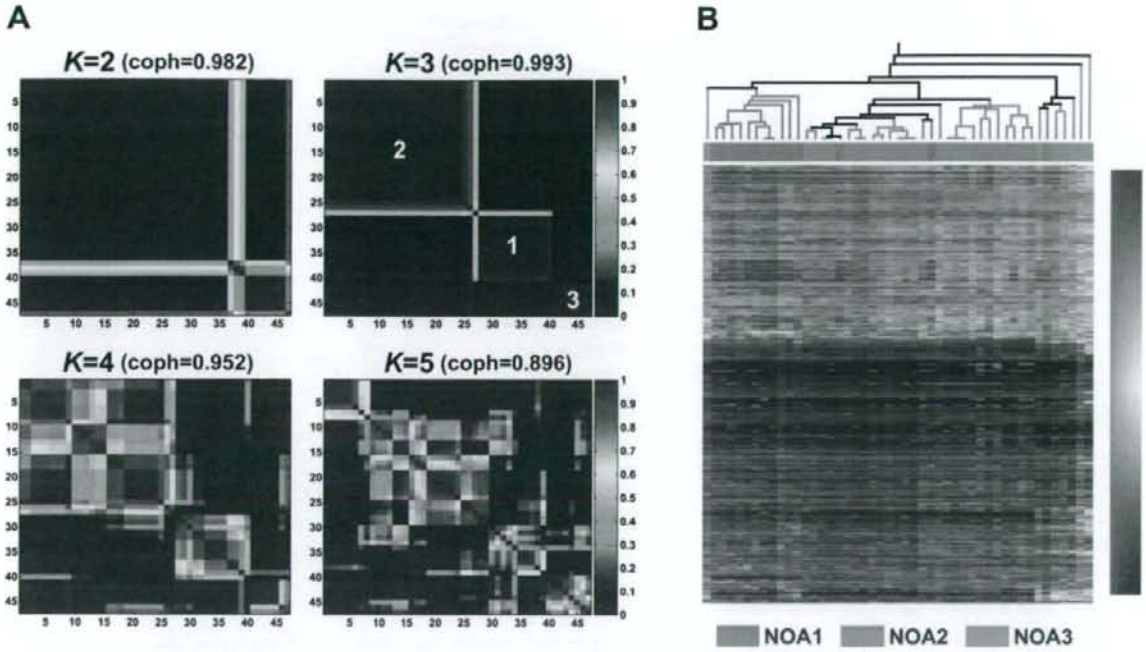

Figure 3. Non-Negative Matrix Factorization (NMF) and Hierarchical Clustering (HC)-based Subclassification of 47 NOA Samples

(A) Reordered consensus matrices averaging 50 connectivity matrices computed at $K = 2$–5 (as the number of subclasses modeled) for the NOA data set comprising of NOA-related target genes. NMF computation and model selection were performed according to Brunet et al. [6] as described in Materials and Methods. According to cophenetic correlation coefficients (coph) for NMF-clustered matrices, the NMF class assignment for $K = 3$ was the most robust.

(B) The HC method incorporated in GeneSpring also was used to classify NOA heterogeneity in testicular gene expression. To display correspondences of subclassification by the two methods, the NMF class assignments for $K = 3$ are shown color-coded; NOA1 (green), NOA2 (pink), and NOA3 (light purple).

doi:10.1371/journal.pgen.0040026.g003

chromosome organization and biogenesis (GO:51276; 7001), sex differentiation (GO: 7548), and response to endogenous stimulus (GO:9719; 6974) occurred after the extraction of 149 transcripts from the NOA-related target gene list (Figure 4). Other features of the 149 transcripts from the gene list (Table S1) were as follows: (1) a high frequency (24.2%) of sex chromosome-linked genes; (2) a high frequency (13.4%) of genes encoding cancer/testis antigens [12,13]; and (3) a moderate frequency (6.7%) of male infertility-related genes. Defect of these genes results in male infertility/subfertility in mice [3,14–16].

Twenty-five of the 149 transcripts showing differences in between-subclass expression displayed elevated expression in NOA, while the others (124 transcripts) had decreased expression (Table S1). The 25 NOA-elevated transcripts accounted only for differences in testicular expression between NOA1 and the other two subclasses, NOA2 and NOA3 (Figure S2; Table S1), suggesting testicular hyperactivity in NOA1 patients. For example, 3β-hydroxysteroid dehydrogenase, encoded by *HSD3B2* and *HSD3B1*, plays a crucial role in biosynthesis of testosterone in Leydig cells [17]. Expression levels of the two transcripts in the NOA1 subclass were higher than those in the NOA2 and NOA3 subclasses, and the expression difference between NOA1 and NOA3 was significant by Tukey's *post hoc* test (Figure S2; Table S1). As the NOA1 subclass showed significantly high LH and slightly low testosterone levels (Table 2), the elevated levels of the two transcripts may be explained by a compensation process for maintaining normal testosterone level. Thus, such enhanced steroidogenesis of the NOA1 subclass might favor, even if only slightly, testicular hyperactivity in NOA1 patients.

On the other hand, among the 124 NOA-decreased transcripts, most transcripts (118/124) showed expression differences between NOA3 and the other two subclasses (Figures S2–S4; Table S1). Expression levels of these transcripts in the NOA3 subclass were similar to those in testis reference RNA (Figures S2–S4), indicating that the NOA3 subclass has a mild defect in spermatogenesis. This notion is supported by the fact that the expression of *INHBB* encoding inhibin β subunit B in the NOA3 subclass is normal while NOA1 and NOA2 subclasses showed low levels, indicating that inhibin β may be a marker of testicular dysfunction, as previously reported [18].

Verification of Between-Subclass Differences in Testicular Expression by Quantitative Real-Time RT-PCR

To evaluate the appropriateness of microarray data on transcripts representing expression differences between NOA subclasses, we selected 53 with high significance ($p < 0.01$, Tukey's *post hoc* test, Figure S1 and Table S1) out of the 149 differentially expressed transcripts and subjected them to real-time RT-PCR analysis. Of the 53 transcripts, the highly

Table 2. Clinical Characteristics of Three Molecular Subclasses of NOA

Group	*n*	Age (Years)	Range	Johnsen's Score*	Range	Serum FSH (mIU/ml)*	Range	Serum LH (mIU/ml)*	Range	Serum T (ng/ml)	Range
OA	11	33.3 ± 8.5	25–57	7.9 ± 1.2	5.1–9	10.1 ± 9.3	3.6–31.4	4.5 ± 2.3	1.3–9.3	4.8 ± 1.7	3.4–7.0
NOA1	13	37.5 ± 6.0	27–52	2.0 ± 1.0[a]	1–4	34.5 ± 11.5[a]	19.0–53.3	13.6 ± 6.0[a]	5.2–20.8	2.8 ± 1.0	1.4–4.7
NOA2	27	34.4 ± 5.6	24–46	2.2 ± 1.1[b]	1–6	28.3 ± 6.4[c]	19.0–39.3	7.2 ± 2.6	2.4–13.0	3.7 ± 1.4	2.2–5.8
NOA3	7	33.0 ± 4.8	26–40	4.0 ± 1.6	2–6.5	22.7 ± 8.8	12.6–28.6	5.9 ± 0.9	5.3–7.0	4.3 ± 2.7	2.0–7.3

The data are represented as mean ± standard deviation.
*$p < 0.01$ (Kruskal-Wallis test between four groups).
[a]$p < 0.01$, NOA1 versus OA (Scheffe's *posthoc* test on Johnsen's score, FSH and LH between four groups).
[b]$p < 0.01$, NOA2 versus OA (Scheffe's *posthoc* test on Johnsen's score, FSH and LH between four groups).
[c]$p < 0.05$, NOA2 versus OA (Scheffe's *posthoc* test on Johnsen's score, FSH and LH between four groups).
FSH, follicle-stimulating hormone; LH, luteinizing hormone; T, testosterone.
doi:10.1371/journal.pgen.0040026.t002

homologous VCX family genes, *VCX*, *VCX2*, and *VCX3A*, were detected with non-specific assay as a mixture of transcripts. Thus, 50 genes and one gene mixture were subjected to real-time RT-PCR. As shown in Figure S5, real-time RT-PCR data of the 51 transcripts were highly correlated with the results of microarray analysis, the squares of correlation coefficients (R^2) ranging from 0.40 (CT45–2) to 0.90 (GAJ). This validation analysis also provided statistically positive evidence on between-subclass differences for all of the 51 transcripts ($p < 0.05$ with Kruskal-Wallis test, data not shown).

Screening of Candidate Genes for Genetic Susceptibility for NOA

One approach to prioritizing candidate genes for genetic susceptibility underlying NOA is to adopt gene expression data from NOA tissues. Genes that show differences in expression level between NOA subclasses regardless of biological impact were selected based on the concept that polymorphic variation in gene expression among unrelated individuals is largely due to polymorphisms in DNA sequence [19,20]. 52 genes having statistical differences in expression ($p < 0.01$, Table S1) were regarded as candidates for allelic association with NOA. Despite the fact that these genes were not selected based on pathological relevance to NOA, genes such as *SYCP3*, *DAZL*, and *INHBB*, which were reported to function in spermatogenesis were included [21–23]. 191 single nucleotide polymorphisms (SNPs) of 42 genes were subjected to allelic association study with 190 NOA patients and 190 fertile men in the first round of screening. Ten genes

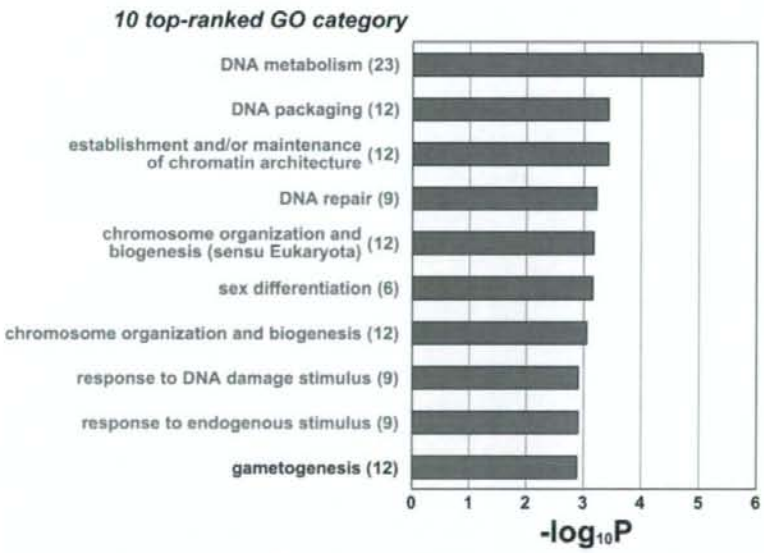

Figure 4. Significant Enrichments of Gene Ontology Categories in GO-based Profiling of 149 Differentially Expressed Transcripts

Grey bars represent *p*-values (expressed as the negative logarithm [base 10]) for the 10 top-ranked GO categories over-represented in the 149 differentially expressed transcripts, using the 2,611 NOA-related target transcripts as a background set of genes for the determination of *p*-values. The actual number of differentially expressed transcripts involved in each category is given in parentheses. In the process of extracting the 149 transcripts from the NOA-related target gene list, sets of genes involved in nine GO categories, marked in magenta, were more condensed because they were not found in the previous 10 top-ranked GO lists of NOA-related target genes (see Table 1 and Figure 2).
doi:10.1371/journal.pgen.0040026.g004

Table 3. Analyses of Allelic Association between 44 SNPs of Seven Candidate Genes and Japanese NOA in Second Round of Initial Screening (380 Cases versus 380 Controls)

Gene	Map	rs ID	Sequence Position[a]	Localization	Variation	MAF		χ^2	Nominal *p*
						Case	Control		
ART3	**4q21.1**	rs9995300	−2520	5′-upstream	A/G	40.7%	34.6%	5.60	0.018
		rs17001357	12048	Intron3	C/T	41.5%	46.4%	3.50	0.061
		rs11097230	19801	Intron3	A/G	32.9%	40.1%	7.79	0.0053
		rs6836703	34283	Intron11	G/A	41.4%	32.8%	11.7	0.00061*
		rs1128864	37726	Exon12-Non-synonymous	T/C	39.3%	33.2%	5.53	0.019
		rs6840007	43329	3′-downstream	A/T	34.5%	28.4%	6.16	0.013
LOC92196	**2q24.1**	rs4254463	−5901	5′-upstream	G/A	18.1%	16.7%	0.46	0.50
		rs908404	2538	Intron1	T/C	17.9%	16.1%	0.69	0.41
		rs9869	11757	Exon3-non-synonymous	C/T	19.7%	14.8%	5.85	0.016
		rs10016	20600	3′-UTR	G/A	9.8%	10.0%	0.00	0.99
NYD-SP20	**17p13.3**	rs3829957	−3785	5′-upstream	C/T	36.0%	36.2%	0.00	0.99
		rs2318035	12022	Intron5	A/G	36.9%	36.1%	0.09	0.77
		rs1488689	22797	Exon6-non-synonymous	A/G	34.8%	34.5%	0.01	0.94
		rs17822627	31572	Exon9-synonymous	T/C	35.6%	34.3%	0.23	0.63
		rs2318033	40646	3′-downstream	A/T	37.3%	36.4%	0.10	0.75
PAGE5	**Xp11.21**	rs2148982	2260	Intron3	G/A	30.9%	30.2%	0.01	0.92
		rs5913800	5332	3′-downstream	A/G	31.0%	29.8%	0.06	0.81
		rs5914276	8924	3′-downstream	C/G	31.4%	29.0%	0.40	0.53
		rs11091394	14424	3′-downstream	A/G	32.4%	28.2%	1.15	0.28
TEX14	**17q22**	rs686425	−7314	5′-upstream	G/A	47.1%	47.3%	0.00	0.99
		rs302874	1420	Intron1	C/T	47.3%	47.2%	0.00	0.99
		rs302865	12439	Intron1	C/T	46.7%	46.3%	0.01	0.93
		rs446613	19870	Intron1	A/C	47.6%	49.1%	0.27	0.60
		rs1631237	34721	Intron2	C/T	46.6%	47.3%	0.05	0.82
		rs302843	41430	Intron2	A/G	46.1%	49.0%	0.87	0.35
		rs2611782	51460	Intron2	C/T	47.5%	47.3%	0.00	0.99
		rs591200	63515	Intron2	C/T	42.8%	41.3%	0.25	0.62
		rs9898626	71197	Intron5	G/C	47.1%	46.4%	0.04	0.85
		rs302854	85804	Intron10	T/C	47.0%	48.0%	0.10	0.75
		rs8072873	100367	Intron15	G/C	24.6%	26.0%	0.30	0.58
		rs6503870	110398	Exon20-non-synonymous	T/C	46.8%	47.0%	0.00	0.95
		rs1267542	114726	Intron22	T/C	45.9%	49.1%	0.94	0.33
		rs3803751	119060	Intron24	T/C	23.5%	25.3%	0.61	0.43
		rs1267545	122507	Intron26	G/A	46.0%	48.1%	0.47	0.49
		rs1974586	128685	Intron29	C/T	23.5%	26.6%	1.67	0.20
		rs2333332	138362	3′-downstream	T/C	48.4%	49.0%	0.04	0.85
		rs714959	140815	3′-downstream	T/C	23.6%	22.6%	0.17	0.68
		rs12453459	145125	3′-downstream	C/T	49.0%	45.6%	0.90	0.34
TKTL1	**Xq28**	rs631	−8147	5′-upstream	G/A	23.4%	18.5%	2.37	0.12
		rs6655282	12986	Intron6	G/A	10.7%	6.8%	3.17	0.075
		rs766420	20834	Intron9	C/G	23.7%	22.7%	0.05	0.82
		rs2872817	24848	3′-UTR	A/G	28.5%	26.8%	0.18	0.67
		rs5945413	30181	3′-downstream	A/T	27.2%	27.0%	0.00	0.99
XAGE5	**Xp11.22**	rs4543711	5279	Intron4	A/G	4.9%	7.9%	2.30	0.13

[a]Nucleotide position from the first nucleotide of exon 1 of each gene.
*Statistically significant (corrected $p = 0.027$) based on Bonferroni-corrected *p*-value.
doi:10.1371/journal.pgen.0040026.t003

(*CTAG1B*, *LOC158812*, *LOC255313*, *MAGEA2*, *PEPP-2*, *TSPY1*, *TSPY2*, *VCX3A*, *VCY*, and *XAGE1*) were not analyzed because no gene-based SNPs with minor allele frequency (MAF) > 0.05 could be found. We identified seven genes (*ART3*, *LOC92196*, *NYD-SP20*, *PAGE5*, *TEX14*, *TKTL1*, and *XAGE5*) with at least one SNP showing a discrepancy in MAF of 5% or greater between cases and controls (Table S2). Forty-four SNPs in the seven genes were subjected to a second round of screening by increasing sample size (380 NOA patients and 380 fertile men). After the two rounds of screenings, only one SNP (rs6836703) of *ART3* (ADP-ribosyltransferase 3) was positively associated with NOA after Bonferroni's correction for multiple testing (Table 3; $\chi^2 = 11.7$, corrected $p = 0.027$).

Allelic Association Study with *ART3*

We focused on *ART3* based on the result of the two rounds of screenings, and identified 38 SNPs with MAF > 0.1 by database search or direct sequencing of the gene. 442 NOA patients (cases) and 475 fertile men (controls) were genotyped. Because we intended in this study to find a common genetic cause for NOA, patients with microdeletions of the Y chromosome at the azoospermia factor (AZF) locus, one of the major causes of NOA [1,2], were not excluded from the cases. However, to characterize the cases in regard to the AZF deletions, we examined the incidence of the deletions in a subset of the cases. Of the 442 NOA patients, 99 were examined by PCR-based screening. Fourteen (14.1 %) of the

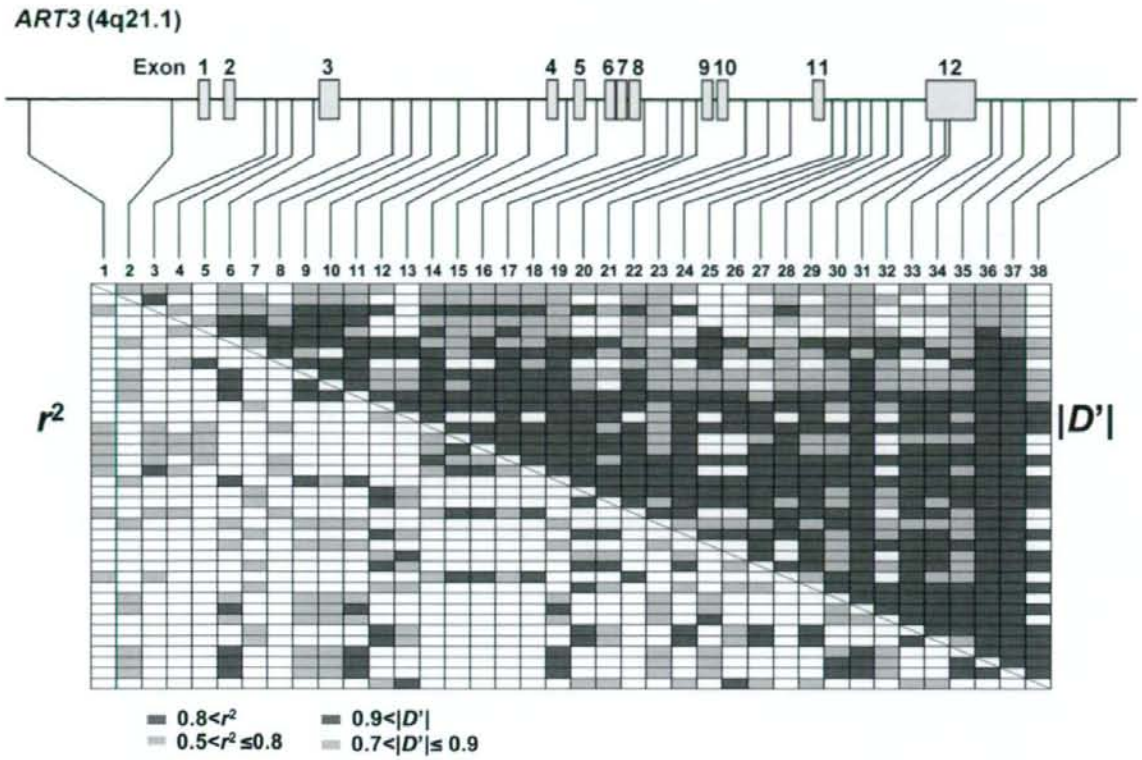

Figure 5. Linkage Disequilibrium Pattern of *ART3*

The gene structure together with the position of 38 SNPs is shown. Pairwise LD coefficients, D' and r^2, of controls were determined and expressed as a block structure. In the schematic block, red boxes indicate pairwise LD of $|D'| > 0.9$ or $r^2 > 0.8$ and pink boxes $0.9 \geq |D'| > 0.7$ or $0.8 \geq r^2 > 0.5$. Blank boxes represent $|D'| \leq 0.7$ or $r^2 \leq 0.5$.

doi:10.1371/journal.pgen.0040026.g005

99 cases examined showed the AZF deletions, and NOA patients with AZFc deletions were most frequent among the 14 cases (data not shown). The overall deletion frequency was comparable to those of other studies [1,2], in which the higher incidence of AZFc deletions also was observed. The clinical characteristics of patients with the AZF deletions did not differ from those of the other NOA patients (data not shown).

Linkage disequilibrium map showed that all of the SNPs of *ART3* were in near complete LD evaluated with D' statistic ($|D'| > 0.7$) in both cases and controls (only controls are displayed in Figure 5). None of the SNPs in the controls showed deviation from Hardy-Weinberg's equilibrium at a threshold of $p < 0.01$ (data not shown). As shown in Table 4, SNPs showing positive associations based on nominal p-values were widely distributed throughout *ART3*. The most significant association was observed with ART3-SNP25 (rs6836703) located in intron 11 of *ART3* ($\chi^2 = 9.16$, nominal $p = 0.0025$, odds ratio [95% CI] = 1.34 [1.11–1.63]). We applied the permutation method for adjustment of multiple testing to avoid a false positive result [24]. A total of four SNPs including ART3-SNP25 met the empirical significance level of $p < 0.05$ (Table 4).

For the haplotype-based association study, we first selected five SNPs (ART3-SNP1, 5, 23, 25, and 28) as tag SNPs captured through LD in *ART3* from 15 SNPs with nominal $p < 0.05$ at a threshold of $r^2 \geq 0.8$ with Tagger software [25]. Haplotype frequencies were inferred using an expectation-maximization (EM) algorithm. After excluding rare haplotypes (frequency < 0.01), association of ART3 haplotypes with NOA was examined in 442 cases and 475 controls. Haplotype H1, the most common haplotype in controls, was under-represented in cases with significance (Figure 6; 26.6% in cases and 35.3 % in controls; $\chi^2 = 15.7$, df = 1, nominal $p = 0.000073$), indicating a protective impact of haplotype H1. After Bonferroni's correction for multiple testing, a protective effect of haplotype H1 was still significant (corrected $p = 0.00080$). Other haplotypes showed no significant difference in frequencies between cases and controls (Figure 6). We also applied a Bayesian algorithm for phasing haplotypes with PHASE version 2.1.1 [26,27]. Regardless of haplotype-phasing methods, haplotype H1 was the most frequent in controls (26.4% in cases and 35.0% in controls), and a significant difference in haplotype H1 frequency between cases and controls was observed (permutation $p < 0.0001$ in global comparison, generated after 10,000 iterations).

Clinical Relevance of the Haplotype Associations

The functional relevance of haplotype H1 in comparison with the clinical data was then explored. Diplotype was

Table 4. Allelic Association of 38 SNPs in *ART3* with NOA in Japanese Population (442 NOA Patients versus 475 Controls)

Number	rs ID	Sequence Position[a]	Localization	Variation	MAF		χ^2	Nominal *p*	Permutation *p*[b]
					Case	Control			
ART3–1	rs13111494	−10376	5′-upstream	T/C	37.7%	43.4%	3.96	0.047	0.36
ART3–2	rs9995300	−2520	5′-upstream	A/G	38.7%	35.8%	1.66	0.20	0.81
ART3–3	rs4859609	3333	intron2	A/G	39.3%	43.2%	2.84	0.092	0.55
ART3–4	rs7666159	3941	intron2	T/C	51.5%	48.7%	1.40	0.24	0.87
ART3–5	rs4859611	5562	intron2	T/C	43.9%	48.8%	4.42	0.035	0.29
ART3–6	rs10007524	7070	intron2	G/A	34.6%	30.7%	3.14	0.077	0.49
ART3–7	rs4859612	9950	intron3	T/G	16.8%	17.8%	0.29	0.59	1
ART3–8	rs17001357	12048	intron3	C/T	40.6%	45.9%	5.13	0.024	0.22
ART3–9	rs4308383	12986	intron3	C/T	35.8%	31.2%	4.24	0.040	0.32
ART3–10	rs17001364	13478	intron3	T/C	36.4%	31.2%	5.47	0.019	0.19
ART3–11	rs7675618	15549	intron3	G/A	35.0%	30.3%	4.33	0.038	0.31
ART3–12	rs4859422	16736	intron3	G/A	23.2%	25.1%	0.88	0.35	0.96
ART3–13	rs4859614	17327	intron3	G/A	32.8%	31.2%	0.51	0.48	1
ART3–14	**rs11097230**	**19801**	**intron3**	**A/G**	**32.5%**	**39.3%**	**8.73**	**0.0031**	**0.040**
ART3–15	rs6829592	23717	intron4	G/A	43.3%	46.0%	1.32	0.25	0.89
ART3–16	rs13131187	25213	intron5	A/G	42.3%	45.1%	1.46	0.23	0.86
ART3–17	**rs17001385**	**26422**	**intron8**	**C/G**	**32.5%**	**39.2%**	**8.84**	**0.0030**	**0.038**
ART3–18	rs12331871	27635	intron8	T/G	39.7%	43.5%	2.57	0.11	0.61
ART3–19	rs17001390	28316	intron8	C/T	34.3%	30.2%	3.49	0.062	0.43
ART3–20	rs12510869	28670	intron8	A/G	23.2%	24.4%	0.36	0.55	1
ART3–21	rs13130116	29976	intron10	C/T	22.6%	24.9%	1.28	0.26	0.90
ART3–22	rs9307076	31256	intron10	G/A	40.3%	43.5%	1.92	0.17	0.75
ART3–23	rs4599438	32278	intron10	A/G	37.5%	31.7%	6.71	0.010	0.11
ART3–24	rs17001409	33549	intron11	T/C	23.8%	25.1%	0.39	0.53	1
ART3–25	**rs6836703**	**34283**	**intron11**	**G/A**	**41.2%**	**34.3%**	**9.16**	**0.0025**	**0.034**
ART3–26	rs4241584	35127	intron11	C/T	30.3%	29.5%	0.13	0.72	1
ART3–27	rs4859423	35158	intron11	T/C	23.7%	25.3%	0.67	0.41	0.99
ART3–28	rs4241586	35506	intron11	T/C	39.7%	44.5%	4.14	0.042	0.33
ART3–29	rs17001416	35935	intron11	G/T	21.6%	22.5%	0.20	0.66	1
ART3–30	rs1128864	37726	exon12-non-synonymous	T/C	38.2%	33.8%	3.72	0.054	0.39
ART3–31	New	37857	exon12–3′-UTR	G/A	34.1%	29.4%	4.58	0.032	0.28
ART3–32	**rs14773**	**37861**	**exon12–3′-UTR**	**A/C**	**45.0%**	**38.1%**	**8.96**	**0.0028**	**0.036**
ART3–33	rs7689378	38491	3′-downstream	A/G	21.7%	23.4%	0.67	0.41	0.99
ART3–34	rs13141802	38730	3′-downstream	G/C	22.3%	24.2%	0.86	0.35	0.97
ART3–35	rs10654	40031	3′-downstream	T/A	34.8%	30.5%	3.64	0.056	0.41
ART3–36	rs7675107	41918	3′-downstream	A/G	33.6%	29.1%	4.19	0.041	0.32
ART3–37	rs6840007	43329	3′-downstream	A/T	34.3%	29.7%	4.42	0.036	0.30
ART3–38	rs4538520	49092	3′-downstream	C/T	33.1%	31.7%	0.39	0.53	1

SNPs in bold show statistical significance and are subjected to haplotype analysis as shown in Figure 6.

[a]Nucleotide position from the first nucleotide of exon 1.

[b]Permutation *p*-values generated by 10,000 iterations. SNPs in bold show statistical significance based on the permutation *p*-values.

doi:10.1371/journal.pgen.0040026.t004

inferred with EM algorithm, and three categories (code 0, 1, and 2) were defined by the number of haplotype H1 carried without counting the other haplotypes, and nonparametric analysis of variance test with clinical data was performed. Serum levels of hormones (LH, FSH, and testosterone), other biochemical and pathophysiological markers, and Johnsen's score were analyzed by Kruskal-Wallis test with a Bonferroni/Dunn *post hoc* test between the three diplogroups. Serum testosterone levels were significantly different among the three groups (Figure 7; $df = 2$, $p = 0.0093$), but there were no significant differences in other clinical markers. *Post hoc* pairwise comparisons revealed that serum testosterone levels were significantly higher in the subgroup having two copies of haplotype H1 than in a subgroup with one or no haplotype H1 ($p = 0.0064$ or $p = 0.0004$, respectively, Figure 7). PHASE-inferred individual diplotypes also revealed a similar correlation between diplogroups of haplotype H1 and serum testosterone levels (data not shown).

ART3 Protein Localization in Azoospermic Testis

ART3 protein expression in azoospermic testes was examined by immunohistochemical analysis. As shown in Figure 8, specific staining of ART3 protein was predominantly observed in spermatocytes in OA testes (Figure 8C–8E) as well as in normal testes from individuals of accidental sudden-death (Figure 8A and 8B). Staining was not observed in other stages of undifferentiated germ cells or Sertoli cells in the seminiferous tubules, or the interstitial tissues such as Leydig cells. On the other hand, we did not detect any ART3 protein in NOA testes with Johnsen's scores ranging from 2 to 3, which showed no spermatocytes, spermatids, or spermatozoa in the seminiferous tubules ($n = 12$ samples; Figure 8F–8H). There was no marked difference in testicular ART3

Haplotype	ART3-SNP#					Freq (EM)		χ^2	*P*-value
	1	5	23	25	28	Control	NOA		
H1	C	C	A	G	C	35.3%	26.6%	15.7	0.000073
H2	T	T	G	A	T	27.5%	28.5%	0.21	0.65
H3	T	T	A	G	T	13.8%	13.4%	0.04	0.84
H4	T	C	A	G	T	7.2%	6.4%	0.47	0.50
H5	C	T	A	A	C	3.0%	4.6%	3.10	0.078
H6	T	C	A	G	C	2.6%	3.2%	0.42	0.52
H7	T	C	G	G	T	1.7%	3.0%	3.22	0.07
H8	C	T	A	G	T	2.0%	1.7%	0.16	0.69
H9	T	T	A	A	C	1.2%	1.7%	0.87	0.35
H10	T	T	A	G	C	1.5%	1.0%	0.62	0.43
Others						4.2%	9.9%		

Figure 6. Haplotype-based Association Study of *ART3*

The expectation-maximization (EM) algorithm [37] was used to infer *ART3* haplotype frequencies with genotyping data of five tag SNPs, ART3-SNP1, 5, 8, 23, 25, and 28 (see Table 4). At the respective SNP sites, red and blue boxes represent minor and major alleles, respectively.

doi:10.1371/journal.pgen.0040026.g006

protein expression among the three *ART3* diplo-groups carrying none, one, or two copies of haplotype H1.

Discussion

Genomic Analysis of NOA

Our investigation was designed to clarify the pathogenesis of NOA using global gene expression analyses of testis samples from NOA patients and to identify genetic susceptibilities underlying NOA from the genes differentially expressed. Large families with multiple generations having NOA cannot be expected due to the nature of infertility, so linkage study is impractical for NOA and has not been reported. Alternatively, allelic association study is a practical approach to identification of genetic susceptibility underlying NOA. Thus far, more than 80 genes have been identified as essential for male infertility in humans and mice [3]. Genes on the Y chromosome were emphasized because of observed microdeletions in patients, and genes such as DAZ and HSFY were examined for possible susceptibility genes [28,29]. Recently, homozygous mutation of the aurora kinase C gene was identified in large-headed multiflagellar polyploid spermatozoa, a rare form of infertility, using homozygosity mapping [30]. In the current study, we applied a novel approach to identify common susceptibility genes for NOA by applying global gene expression analysis of NOA testes. Based on the hypothesis that a common variant of a susceptibility gene has resulted in altered expression in tissues relevant to disease etiology [31], we first elucidated the gene expression profile in testes of NOA patients and characterized the genetic pathways that were either under-expressed or over-expressed. Because spermatogenesis is a complex differentiation process, NOA could result from a defect at any stage of the process. Thus, gene expression profiling of NOA tissues might well be confounded by the difficulty of discerning the differential stage and the pathological status. Feig et al. [4] examined stage-specific gene expression profiles in human NOA patients after classification on the basis of Johnsen's score. The testis tissues were classified into four groups showing Sertoli-cell only syndrome, meiotic arrest, testicular hypospermia, and testicular normospermia, corresponding to Johnsen's score 2, 5, 8, and 10, respectively, and stage-specific differential gene expression was monitored. We sought to identify susceptibility genes underlying NOA that could affect any stage of spermatogenesis. Testis samples subgrouped according to Johnsen's score in advance might identify genes affecting multiple stages of spermatogenesis. Therefore, we globally subgrouped the samples at diverse stages of differentiation using an NMF method for reducing multidimensionality that is appropriate for application to high dimensional biological data. The NMF method subgrouped three classes, NOA1, NOA2, and NOA3, which also were unequivocally subgrouped by the HC approach (Figure 3). Notably, NOA1 and NOA2 represent a pathologically similar type showing low Johnsen's score, but were subclassified because of their distinct gene expression pattern. NOA1 and NOA2 showed differences in LH, FSH, and testosterone levels, thus establishing meaningful biological significance of the sub-classes (Table 2).

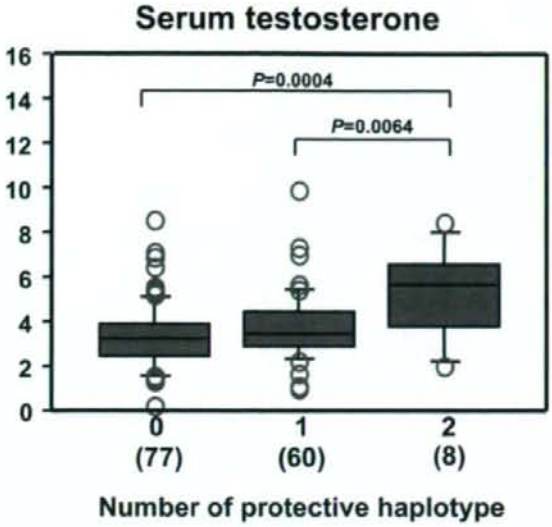

Figure 7. Diplotype-Specific Differences in Serum Testosterone Levels in NOA Patients

Three diplo-groups (code 0, 1, and 2) were defined by the number of *ART3* haplotype H1 carried. The serum testosterone levels were significantly different among the three groups (Kruskal-Wallis; df = 2, $p = 0.0093$) by Bonferroni/Dunn *post hoc* test.

doi:10.1371/journal.pgen.0040026.g007

Genetic Susceptibility to NOA

In the current study, we adopted a novel approach to select candidate susceptibility genes for NOA. Global gene expression analyses were performed on NOA testes, and 52 genes were selected according to differential gene expression between NOA subclasses with a strict statistical criterion ($p < 0.01$ with Tukey's *post hoc* test). Despite the fact that our selection criteria relied only on data regarding differences in gene expression and did not include any biological assumptions, many of the genes were related to spermatogenesis based on Gene Ontology analyses (Figure 4; Table 1). 191 SNPs of 42 genes were screened, and only one gene, *ART3*, showed a positive association after the two rounds of screening. Multiple SNPs of *ART3* were significantly associ-

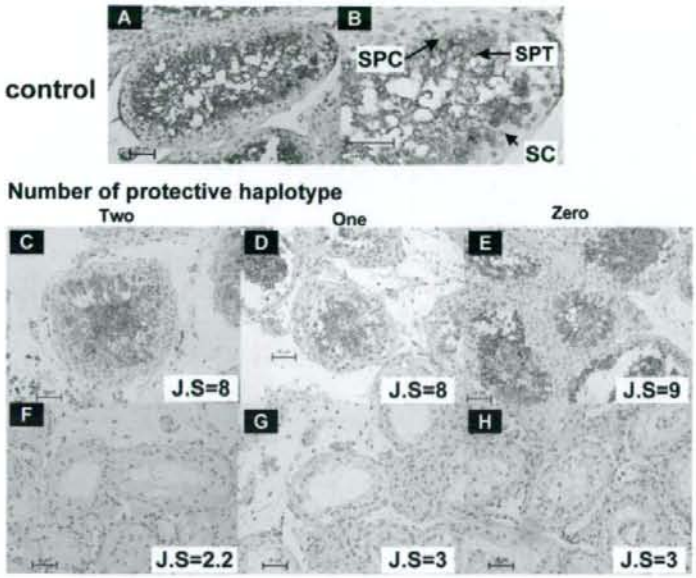

Figure 8. Immunohistochemical Analysis of ART3 Expression in Human Testes

Representative seminiferous tubules in testicular sections from normal controls (A, B), OA (C–E), and NOA patients (F–H) are shown. Arrows indicate spermatocytes (SPC); spermatids (SPT); and Sertoli cells (SC) (B). ART3 protein was immunostained with anti-ART3 antibody; ART3-positive spermatocytes (SPC) are noted as brown staining cells (A–E). No marked differences in testicular ART3 expression among the three ART3 diplo-groups carrying none, one, or two copies of the protective haplotype H1were observed in OA (C–E) and NOA (F–H) patients. Magnification is 60× except in (B) (120×).

doi:10.1371/journal.pgen.0040026.g008

ated with NOA, the most significant association being observed with ART3-SNP25 (rs6836703, nominal $p = 0.0025$, permutation $p = 0.034$; Table 4). We also detected a protective haplotype, H1, which was the most common form and was strongly associated with NOA (nominal $p = 0.000073$, corrected $p = 0.00080$, Figure 6). In addition, diplotype analysis showed that individuals carrying at least one haplotype H1 showed an elevated plasma testosterone level (Figure 7).

Functional Relevance of ART3 in the Pathogenesis of NOA

ART3 is a member of the mono-ADP-ribosyltransferase family genes. The biological function of ART3 remains obscure, as ART3 does not display any detectable arginine-specific transferase activity due to lack of the active site motif (R-S-EXE) that is essential for catalytic activity. Since differentiation of stage-specific expression of ART3 in testis has been reported, protein expression being exclusively present in spermatocytes but absent in spermatozoa [32], a genetic variation of *ART3* might well lead to a functional defect in the process of spermatogenesis. Haplotype H1 of *ART3*, comprising all of the disease-protective alleles at the respective SNP sites, was under-represented in the patients. However, functional disturbance associated with haplotype H1 is so far undetermined despite the fact that several experiments designed to demonstrate haplotype-specific differences in expression level have been performed. Thus, it is possible that this haplotype represents fine tuning that maintains normal maturation of spermatocytes and improves the efficiency of spermatogenesis.

In conclusion, genome-wide gene expression analyses identified differentially expressed genes of NOA subclasses, and *ART3* was identified as a susceptibility gene underlying NOA. This genetic study constitutes only first-stage evidence of association because only Japanese individuals were included, so further replication in independent case-control samples is required to confirm the role of the *ART3* haplotype in genetic risk for NOA. Although further functional evidence is also required, these results provide insight into the pathoetiology of NOA as well as reproductive fitness at the molecular level, and suggest a target for therapy.

Materials and Methods

Participants. Testicular biopsy specimens for microarray analysis were obtained from 47 Japanese patients (aged from 24 to 52 years) with NOA and 11 (aged from 22 to 57 years) with OA, each of whom also underwent testicular sperm extraction (TESE) for assisted reproduction and/or diagnostic biopsy for histological examination. The biopsies for microarray analysis and histological examination were mainly sampled from unilateral, multiple testicular sites in the respective patients. Each patient was first assigned to azoospermia by showing no ejaculated spermatozoa in a semen examination. Subsequently, OA was defined as follows: (1) motile spermatozoa were sampled from microsurgical epididymal sperm aspiration (MESA), or (2) a considerable number of mature spermatozoa was sampled from TESE. NOA was tentatively defined as having no epididymal and/or testicular spermatozoa. The degree of spermatogenic defect was histologically evaluated according to Johnsen's score [11]. At least three biopsies from the same individual were taken, and the average Johnsen's scores in the NOA and OA groups ranged from 1 to 6.5 and from 5.1 to 9, respectively. In most patients, preoperative levels of serum follicle-stimulating hormone (FSH), leutenizing hormone (LH), and total testosterone were measured. The infertile male patients who visited Niigata University, Tachikawa Hospital, and St. Mother's Hospital received a routine semen examination according to 1999 WHO criteria. Based on this analysis, sperm were counted

and the patients who had no ejaculated sperms were enrolled for a case-control association study. In total, 442 patients were ascertained to have NOA. In the current study, azoospermia patients with varicocele, ejaculatory dysfunction, endocrinopathy, or histologically examined OA as defined above were excluded. 475 fertile men having no specific clinical record were recruited in Niigata University. The ethics committees of Niigata University, Tachikawa Hospital, St. Mother's Hospital, and Tokai University approved the study protocols, and each participant gave written informed consent. Genomic DNA was prepared from blood white cells by Dneasy (Qiagen, Tokyo, Japan) or salivas by phenol/chloroform extraction.

To examine microdeletion of the Y chromosome in a subset of NOA patients, PCR-based diagnostic technique was used as follows: PCR amplifications with fluorescence (FAM or HEX)-labeled primers were performed to obtain fragments encompassing each of 13 STS markers in and around azoospermia factor (AZF) regions of the Y chromosome (in AZFa: SY83, SY95 and SY105; in AZFb: SY118, G65320, SY126 and SY136; in AZFc: SY148, SY149, SY152, SY283 and SY1291; in the heterochromatin distal to AZFc: SY166). Primer sequences and PCR conditions are available from the authors on request. PCR-amplified fragments were run on the ABI PRISM 3100 Genetic Analyzer (Applied Biosystems, Tokyo, Japan), and Y-chromosome microdeletion was determined with GENESCAN software (Applied Biosystems).

Microarray analysis of testis samples. Total RNA from testicular biopsy was extracted using TRIzol reagent (Invitrogen, Carlsbad, CA, USA) and quantity and quality of the extracted RNA were examined with 2100 Bioanalyzer (Agilent Technologies, Palo Alto, CA, USA) using RNA 6000 Nano LabChip (Agilent Technologies). Human Testis Total RNA (BD Biosciences, San Jose, CA, USA), a histologically normal testicular RNA pooled from 39 Caucasians, was used as a common reference in two-color microarray experiments.

For fluorescent cRNA synthesis, high-quality total RNA (150 ng) was labeled with the Low RNA Input Fluorescent Linear Amplification Kit (Agilent Technologies) according to the manufacturer's instructions. In this procedure, cyanine 5-CTP (Cy5) and cyanine 3-CTP (Cy3) (PerkinElmer, Boston, MA, USA) were used to generate labeled cRNA from the extracted patient RNA and the reference RNA, respectively. Labeled cRNAs (0.75 μg each) from one patient and the common reference were combined and fragmented in a hybridization mixture with the *In Situ* Hybridization Kit Plus (Agilent Technologies). The mixture was hybridized for 17 hours at 65°C to the Agilent Human 1A(v2) Oligo Microarray, which carries 60-mer probes to 18,716 human transcripts. After hybridization, the microarray was washed with SSC buffer, and then scanned in Cy3 and Cy5 channels with the Agilent DNA Microarray Scanner model G2565AA (Agilent Technologies). Signal intensity per spot was generated from the scanned image with Feature Extraction Software ver7.5 (Agilent Technologies) in default setting. Spots that did not pass quality control procedures were flagged and removed for further analysis.

The Lowess (locally weighted linear regression curve fit) method was applied to normalize the ratio (Cy5/Cy3) of the signal intensities generated in each microarray with GeneSpring GX 7.3 (Agilent Technologies). Compared with the expression level of reference RNA, the NOA group, with expression undergoing a 2-fold mean change or more was extracted; the OA group comprised transcripts showing less than 2-fold mean expression change (Figure 1A). Of the transcripts included in both groups, only those with a statistically significant difference in expression between NOA and OA testes (based on lowess-normalized natural log[Cy5/Cy3], Bonferroni's corrected $p < 0.05$) were counted as NOA-related target genes. To elucidate the molecular subtypes of NOA, we adopted the non-negative matrix factorization (NMF) algorithm, which has been recently introduced to analysis of gene expression data [5,6]. For this analysis, a complete dataset without missing values was generated from raw values of Cy5 intensities for the NOA-related target genes in the NOA samples, and used to clarify NOA heterogeneity using three M-files (available from the following URL; http://www.broad.mit.edu/cgi-bin/cancer/publications/pub_paper.cgi?mode=view&paper_id=89) for MATLAB (Mathworks, Natick, MA, USA). According to the subclassification of NOA samples, transcripts differentially expressed between NOA subclasses were determined by one-way ANOVA, followed by Tukey's *post hoc* test in GeneSpring GX. For multiple test corrections in this statistical analysis, we used the Benjamini-Hochberg procedure [33] of controlling the false discovery rate (FDR) at the level of 0.05 or 0.01. To analyze which categories of Gene Ontology were statistically overrepresented among the gene lists obtained, we used GO Browser, an optional tool in GeneSpring GX, where the statistical significance was determined by Fisher's exact test. The microarray data reported in this paper have been deposited in the Gene Expression Omnibus (GEO, http://www.ncbi.nlm.nih.gov/geo/) database, and are accessible through GEO Series accession number GSE9210.

Quantitative real-time RT-PCR analysis for validation of between-subclass differences in gene expression. Quantitative real-time RT-PCR analysis was used to verify the microarray data on 53 transcripts representing differential expressions between NOA subclasses with high significance ($p < 0.01$). Among 53 transcripts, VCX (NM_013452), VCX2 (NM_016378), and VCX3A (NM_016379) were examined as a single transcript because sequence homologies between the three transcripts prevented development of appropriate assays for discrimination. Testicular total RNA (1 μg) subjected to microarray analysis was used as a template in first-strand cDNA synthesis with SuperScript III First-Strand Synthesis System (Invitrogen). Each single-stranded cDNA was diluted one-tenth for a subsequent real-time RT-PCR using SYBR *Premix Ex Taq* (Perfect Real Time) (TAKARA BIO, Otsu, Japan) on the ABI PRISM 7900HT Sequence Detection System (Applied Biosystems) according to the manufacturer's instructions. The PCR primers for 43 transcripts showing between-subclass differences with high significance and *GAPDH* were designed and synthesized by TAKARA BIO Inc., or QIAGEN GmbH (as the QuantiTect Primer Assay). In the real-time RT-PCR analysis for the nine remaining transcripts, we used TaqMan Gene Expression Assays (Applied Biosystems) with TaqMan Universal PCR Master Mix (No AmpErase UNG version) according to the manufacturer's instructions (Applied Biosystems). The detailed information on the primer sequences used and/or the assay system selected are summarized in Table S3. A relative quantification method [34] was used to measure the amounts of the respective genes in NOA testes, normalized to *GAPDH* as an endogenous control, and relative to Human Testis Total RNA (BD Biosciences) as a reference RNA. Statistical significance between NOA subclasses was determined by Kruskal-Wallis test, followed by multiple comparisons; $p < 0.05$ was considered significant.

SNP selection of candidate genes for NOA and genotyping. Based on gene expression data of NOA testes, we selected 52 genes (encoding 53 transcripts) as candidates for genetic susceptibilities underlying NOA. SNPs of the candidate genes with minor allele frequency (MAF) > 0.05 were obtained from the NCBI dbSNP database (http://www.ncbi.nlm.nih.gov/SNP/), and applied to an initial screening. Of the 52 candidate genes, 10 genes (CTAG1B, LOC158812, LOC255313, MAGEA2, PEPP-2, TSPY1, TSPY2, VCX3A, VCY, and XAGE1) were excluded from the initial screening because gene-based SNPs with MAF > 0.05 were not found in the public SNP database. A total of 191 SNPs of 42 genes were genotyped in the screening with TaqMan SNP Genotyping Assays on the ABI PRISM 7900HT Sequence Detection System (Applied Biosystems). 190 NOA patients (cases) and 190 fertile men (controls) were genotyped in the first round screening. For genes with at least one SNP showing a discrepancy in MAF of 5% or greater between cases and controls, the sample size was increased to 380 cases and 380 controls in the second round.

After two rounds of initial screening, additional SNPs of *ART3* were selected from dbSNP or identified by direct sequencing of all 12 exons of the gene (Ensemble transcript ID ENST00000355810) and splice acceptor and donor sites in the intron using the genomic DNAs from 95 infertile patients as PCR templates. A total of 38 SNPs of *ART3* were finally genotyped on 442 cases and 475 controls by TaqMan SNP Genotyping Assays or by direct sequencing with BigDye Terminators v3.1 Cycle Sequencing Kit (Applied Biosystems) on ABI PRISM 3700 DNA analyzer.

Statistical analyses in association study. Pairwise linkage disequilibrium (LD), using the standard definition of D' and r^2 [35,36], was measured with SNPAlyze v5.0 software (DYNACOM, Mobara, Japan). To construct *ART3* haplotypes in phase-unknown samples, tag SNPs of *ART3* were selected with Tagger software [25], incorporated in the Haploview. The expectation-maximization (EM) algorithm [37] and PHASE version 2.1.1 [26,27] was used to infer haplotype frequencies and individual diplotypes for *ART3*. Differences in allelic and haplotype frequencies were evaluated using a case-control design with the chi-square test. For an adjustment of multiple testing, we applied a permutation method with Haploview version 3.32 software, or Bonferroni's method to determine corrected *p*-values.

To investigate association of the *ART3* diplotype with clinical phenotypes such as serum hormone levels, differences among the three categories (code 0, 1, and 2), defined by the number of the most significant haplotype, were statistically examined by Kruskal-Wallis test, followed by Bonferroni/Dunn *post hoc* test (StatView version 5.0, SAS Institute, Cary, NC, USA).

Immunohistochemistry. To examine cellular localization of ART3

protein in azoospermic testes, testicular biopsy specimens from 15 OA and 12 NOA patients were subjected to immunohistochemistry. Four postmortem testicular tissues of accidental sudden-deaths were used as normal controls. The testicular tissues were fixed in 10% buffered formalin and embedded in paraffin. Cryosections (3 μm thickness) were pre-incubated with the Histofine Antigen-Retrieval Solution (1:10 dilution; Nichirei Bioscience, Tokyo, Japan) for 10 minutes at 95 °C. The sections were then incubated with primary ART3 antibody (1:4,000; Abnova, Taipei, Taiwan), then with IgG2b isotype (1:4,000; MBL International, Woburn, USA) for 60 minutes at room temperature. After washing with PBS, the sections were incubated with the Histofine Simple Stain Max-PO (Multi) (1:5 dilution; Nichirei Bioscience) for 30 minutes at room temperature, and then reacted with DAB (Nichirei Bioscience) for 10 minutes at room temperature. Haematoxylin was used for counterstaining.

Supporting Information

Figure S1. Statistical Analysis Reveals Transcripts Differentially Expressed among Three NOA Subclasses

Venn diagram summaries show the number of transcripts differentially expressed with significance by Tukey's *post hoc* test in each comparison (see Table S1)

Found at doi:10.1371/journal.pgen.0040026.sg001 (694 KB EPS).

Figure S2. Comparisons of Expression Levels of 149 Transcripts Expressed Differentially between Three NOA Subclasses in Microarray Analysis (Part I)

Natural log-transformed normalized ratios of NOA to testis reference (y-axes) were subjected to statistical analysis, as described in Materials and Methods. Each column represents mean ± standard error of the mean. The 53 transcripts with highly significant ($p < 0.01$, Tukey test) differences between the three NOA subclasses are shown in red.

Found at doi:10.1371/journal.pgen.0040026.sg002 (773 KB EPS).

Figure S3. Comparisons of Expression Levels of 149 Transcripts Expressed Differentially between Three NOA Subclasses in Microarray Analysis (Part II)

Natural log-transformed normalized ratios of NOA to testis reference (y-axes) were subjected to statistical analysis, as described in Materials and Methods. Each column represents mean ± standard error of the mean. The 53 transcripts with highly significant ($p < 0.01$, Tukey test) differences between the three NOA subclasses are shown in red.

Found at doi:10.1371/journal.pgen.0040026.sg003 (798 KB EPS).

Figure S4. Comparisons of Expression Levels of 149 Transcripts Expressed Differentially between Three NOA Subclasses in Microarray Analysis (Part III)

Natural log-transformed normalized ratios of NOA to testis reference (y-axes) were subjected to statistical analysis, as described in Materials and Methods. Each column represents mean ± standard error of the mean. The 53 transcripts with highly significant ($p < 0.01$, Tukey test) differences between the three NOA subclasses are shown in red.

Found at doi:10.1371/journal.pgen.0040026.sg004 (822 KB EPS).

Figure S5. Correlations of Testicular Gene Expression Evaluated by Microarray and Quantitative Real-Time RT-PCR Analyses

Expression levels of 51 transcripts with highly significant ($p < 0.01$) differences in expression among the three NOA subclasses were quantified by real-time RT-PCR method as described in Material and Methods. Squares of correlation coefficients (R^2) for the respective transcripts were calculated between normalized expression ratios of NOA to testis reference in microarray data (*x*-axes) and the corresponding ratios obtained by real-time RT-PCR analysis (*y*-axes)

Found at doi:10.1371/journal.pgen.0040026.sg005 (1.7 MB EPS).

Table S1. 149 Transcripts Representing Statistically Significant ($p < 0.05$) Differences in Testicular Expression between Three NOA Subclasses

Found at doi:10.1371/journal.pgen.0040026.st001 (68 KB XLS).

Table S2. Comparison of Minor Allele Frequencies (MAFs) at 191 SNPs of 42 Genes between 190 Infertile Patients and 190 Fertile Males (First Round of Initial Screening)

Found at doi:10.1371/journal.pgen.0040026.st002 (415 KB DOC).

Table S3. Quantitative Real-time RT-PCR Assays for 51 Transcripts Representing Highly Significant Differences between NOA Subclasses

Found at doi:10.1371/journal.pgen.0040026.sg003 (30 KB XLS).

Acknowledgments

We thank tissue and DNA donors and supporting medical staff for making this study possible. We are grateful to M. Takamiya, Y. Sakamoto, and K. Otaka for their technical assistance.

Author contributions. AT, KT, and II conceived and designed the experiments. HO and AT performed the experiments and analyzed the data. AT, KS, KT, and II contributed reagents/materials/analysis tools. HO, AT, and II wrote the manuscript. All authors contributed to editing the manuscript. HO and AT have joint authorship of this manuscript.

Funding. This work was supported in part by a Grant-in-Aid for scientific research from the Japanese Ministry of Education, Science, Sports, and Culture; a Grant-in-Aid for the Promotive Operations of Scientific Research on Children and Families from the Japanese Ministry of Health, Labor and Welfare; and 2007 Tokai University School of Medicine Research Aid.

Competing interests. The authors have declared that no competing interests exist.

References

1. Pryor JL, Kent-First M, Muallem A, Van Bergen AH, Nolten W, et al. (1997) Microdeletions in the Y chromosome of infertile men. N Eng J Med 336: 534–539.
2. Krausz C, Rajpert-de Meyts E, Frydelund-Larsen L, Quintana-Murci L, McElreavey K, et al. (2001) Double-blind Y chromosome microdeletion analysis in men with known sperm parameters and reproductive hormone profiles: microdeletions are specific for spermatogenic failure. J Clin Endocrinol Metab 86: 2638–2642.
3. Matzuk MM, Lamb DJ (2002) Genetic dissection of mammalian fertility pathways. Nat Cell Biol 4 (Supplement): S41–S49.
4. Feig C, Kirchhoff C, Ivell R, Naether O, Schulze W, et al. (2006) A new paradigm for profiling testicular gene expression during normal and disturbed human spermatogenesis. Mol Hum Reprod 13: 33–43.
5. Kim PM, Tidor B (2003) Subsystem identification through dimensionality reduction of large-scale gene expression data. Genome Res 13: 1706–1718.
6. Brunet JP, Tamayo P, Golub TR, Mesirov JP (2004) Metagenes and molecular pattern discovery using matrix factorization. Proc Natl Acad Sci U S A 101: 4164–4169.
7. Pascual-Montano A, Carmona-Saez P, Chagoyen M, Tirado F, Carazo JM, et al. (2006) bioNMF: a versatile tool for non-negative matrix factorization in biology. BMC Bioinformatics 7: 366.
8. Churchill GA (2002) Fundamentals of experimental design for cDNA microarrays. Nat Genet 32 (Supplement): 490–495.
9. Micic S (1983) The effect of the gametogenesis on serum FSH, LH and prolactin levels in infertile men. Acta Eur Fertil 14: 337–340.
10. Yaman O, Ozdiler E, Seckiner I, Gogus O (1999) Significance of serum FSH levels and testicular morphology in infertile males. Int Urol Nephrol 31: 519–523.
11. Johnsen SG (1970) Testicular biopsy score count—a method for registration of spermatogenesis in human testes: normal values and results in 335 hypogonadal males. Hormones 1: 2–25.
12. Scanlan MJ, Simpson AJ, Old LJ (2004) The cancer/testis genes: review, standardization, and commentary. Cancer Immun 4: 1.
13. Simpson AJ, Caballero OL, Jungbluth A, Chen YT, Old LJ (2005) Cancer/testis antigens, gametogenesis and cancer. Nat Rev Cancer 5: 615–625.
14. Crackower MA, Kolas NK, Noguchi J, Sarao R, Kikuchi K, et al. (2003) Essential role of Fkbp6 in male fertility and homologous chromosome pairing in meiosis. Science 300: 1291–1295.
15. Spruck CH, de Miguel MP, Smith AP, Ryan A, Stein P, et al. (2003) Requirement of Cks2 for the first metaphase/anaphase transition of mammalian meiosis. Science 300: 647–650.
16. Greenbaum MP, Yan W, Wu MH, Lin YN, Agno JE, et al. (2006) TEX14 is essential for intercellular bridges and fertility in male mice. Proc Natl Acad Sci U S A 103: 4982–4987.
17. Hedger MP, de Kretser DM (2000) Leydig cell function and its regulation. In: McElreavey K, editor. The genetic basis of male infertility. Berlin and Heidelberg: Springer-Verlag. pp. 69–110.
18. Nagata Y, Fujita K, Banzai J, Kojima Y, Kasima K, et al. (2005) Seminal plasma inhibin-B level is a useful predictor of the success of conventional testicular sperm extraction in patients with non-obstructive azoospermia. J Obstet Gynaecol Res 31: 384–388.
19. Cheung VG, Conlin LK, Weber TM, Arcaro M, Jen KY, et al. (2002) Natural